Journal Pre-proofs

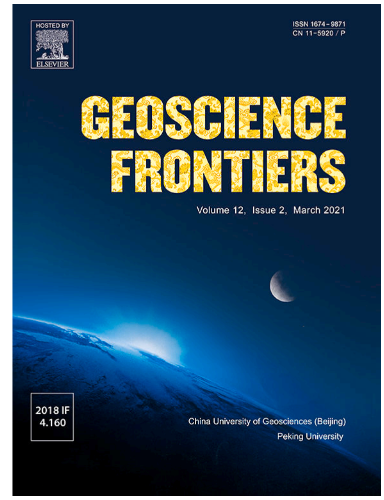

Research Paper

Earth's tectonic and plate boundary evolution over 1.8 billion years

Xianzhi Cao, Alan S. Collins, Sergei Pisarevsky, Nicolas Flament, Sanzhong Li, Derrick Hasterok, R. Dietmar Müller

PII: S1674-9871(24)00146-4
DOI: https://doi.org/10.1016/j.gsf.2024.101922
Reference: GSF 101922

To appear in: *Geoscience Frontiers*

Received Date: 19 January 2024
Revised Date: 23 July 2024
Accepted Date: 28 August 2024

Please cite this article as: X. Cao, A.S. Collins, S. Pisarevsky, N. Flament, S. Li, D. Hasterok, R. Dietmar Müller, Earth's tectonic and plate boundary evolution over 1.8 billion years, *Geoscience Frontiers* (2024), doi: https://doi.org/10.1016/j.gsf.2024.101922

Research Paper

Earth's tectonic and plate boundary evolution over 1.8 billion years

Xianzhi Cao[a,*], Alan S. Collins[b], Sergei Pisarevsky[c], Nicolas Flament[d], Sanzhong Li[a], Derrick Hasterok[b], R. Dietmar Müller[e]

[a] Frontiers Science Center for Deep Ocean Multispheres and Earth System; Key Lab of Submarine Geosciences and Prospecting Techniques, MOE and College of Marine Geosciences, Ocean University of China, Qingdao 266100, China.

[b] Tectonics and Earth Systems & Mineral Exploration Cooperative Research Centre, School of Physics, Chemistry and Earth Sciences, The University of Adelaide, Adelaide, SA 5005, Australia.

[c] Earth Dynamics Research Group, School of Earth and Planetary Sciences, Curtin University, WA 6845, Australia.

[d] GeoQuEST Research Centre, School of Earth and Environmental Sciences, University of Wollongong, Northfields Avenue, NSW 2522, Australia.

[e] EarthByte Group, School of Geosciences, The University of Sydney, NSW 2006, Australia.

***Corresponding author:** Xianzhi Cao

Email: caoxianzhi@ouc.edu.cn; caoxianzhi1990@163.com

Abstract: Understanding the intricate relationships between the solid Earth and its surface systems in deep time necessitates comprehensive full-plate tectonic reconstructions that include evolving plate boundaries and oceanic plates. In particular, a tectonic reconstruction that spans multiple supercontinent cycles is important to understand the long-term evolution of Earth's interior, surface environments and mineral resources. Here, we present a new full-plate tectonic reconstruction from 1.8 Ga to present that combines and refines three published models: one full-plate tectonic model spanning 1 Ga to present and two continental-drift models focused on the late Paleoproterozoic to Mesoproterozoic eras. Our model is constrained by geological and geophysical data, and presented as a relative plate motion model in a paleomagnetic reference frame. The model encompasses three supercontinents, Nuna (Columbia), Rodinia, and Gondwana/Pangea, and more than two complete supercontinent cycles, covering ~40% of the Earth's history. Our refinements to the base models are focused on times before 1.0 Ga, with minor changes for the Neoproterozoic. For times between 1.8 Ga and 1.0 Ga, the root mean square speeds for all plates generally range between 4 cm/yr and 7 cm/yr (despite short-term fast motion around 1.1 Ga), which are kinematically consistent with post-Pangean plate tectonic constraints. The time span of the existence of Nuna is updated to between 1.6 Ga (1.65 Ga in the base model) and 1.46 Ga based on geological and paleomagnetic data. We follow the base models to leave Amazonia/West Africa separate from Nuna (as well as Western Australia, which only collides with the remnants of Nuna after initial break-up), and South China/India separate from Rodinia. Contrary to the concept of a "boring billion", our model reveals a dynamic geological history between 1.8 Ga and 0.8 Ga, characterized by supercontinent assembly and breakup, and continuous accretion events. The model is publicly accessible, providing a framework for future refinements and facilitating deep time studies of Earth's system. We suggest that the model can serve as a valuable working hypothesis, laying the groundwork for future hypothesis testing.

Keywords: Plate reconstruction, Nuna, Supercontinent, Proterozoic, Paleogeography

Handling Editor: R. Damian Nance

1. Introduction

The motion and recycling of tectonic plates shapes the long-term evolution of the Earth's surface and affects deep mantle convection patterns (e.g. Nance et al., 2014; Flament et al., 2022; Müller et al., 2022a). Reconstructing past plate tectonic configurations (Seton et al., 2023) is required to understand the deep-time controls and interactions between the solid Earth and the climate (e.g. Goddéris et al., 2017; Gernon et al., 2021; Mills et al., 2023), the carbon cycle (e.g. Müller et al., 2022b; Goddéris et al., 2023), the water cycle (Karlsen et al., 2019), the spatial and temporal distribution of critical mineral deposits (e.g. Wrobel-Daveau et al., 2022), the nutrient flux required to power biosphere evolution (e.g. Brocks et al., 2017; Mukherjee and Large, 2020; Cox et al., 2022; Spencer, 2022; Zhu et al., 2022) and plate tectonic controls on paleogeography (e.g. Merdith et al., 2017b; Collins et al., 2021).

Supercontinents, resulting from the aggregation of most continental crust into a single landmass, represent a fascinating phenomenon of plate tectonics. Two well-known Proterozoic supercontinents, Rodinia and Nuna (Fig. 1), have been subjects of extensive research, although their configurations are still the subject of much debate. The assembly of Rodinia was completed mainly through global orogenesis at the end of the Mesoproterozoic (Evans, 2013). Major building blocks of the previous supercontinent Nuna (Hoffman, 1997), also sometimes named Columbia (Rogers and Santosh, 2002), or Hudsonland (Williams et al., 1991), were formed over a protracted period of time spanning the middle to late Paleoproterozoic (Zhao et al., 2002). Recently, geochronological and paleomagnetic studies have been interpreted to constrain the assembly of the core of Nuna, between western North America and eastern Australia, to ~1.6 Ga (Pourteau et al., 2018; Kirscher et al., 2022).

In the absence of preserved ocean floor, reconstructions of the pre-Pangean Earth rely on geological evidence preserved within the continents. Age-equivalent orogenic belts, dyke intrusions, comparable rift histories and provenance records, are crucial data to establish past relationships between continents, or constrain supercontinent configurations, especially for early studies (Rogers and Santosh, 2002; Zhao et al., 2002). With the accumulation of paleomagnetic data in recent years, significant progress has been made in building quantitative kinematic reconstructions through time. Early kinematic reconstructions focused on modelling continental motions without plate boundaries or oceanic plates (Li et al., 2008; Eglington et al., 2013; Pisarevsky et al., 2014) due to the lack of data and technical difficulties in building reconstructions with time-dependent plate geometries.

Plate tectonic reconstructions that include evolving global plate boundaries, also called full-plate reconstructions (Merdith et al., 2017a), have become possible with the development of the software GPlates (Müller et al., 2018). Several such models have been published over the last decade, covering different time periods and based on varying geological or geophysical datasets (Merdith et al., 2021). The earliest of these are for post-Pangea times (Seton et al., 2012; Müller et al., 2016), and later for the Paleozoic (e.g. Domeier and Torsvik, 2017). Merdith et al. (2021) created a breakthrough model spanning 1 Ga to present, building on, and integrating, previous models. Li et al. (2023) published a model for the period of 2.0 Ga to 540 Ma, modifying and extending their previous Rodinia model (Li et al., 2008) further back in time and incorporating elements of evolving plate margins. Compared to the relatively high accuracy of post-Pangean full plate models, constrained by preserved oceanic lithosphere, pre-Pangean full-plate reconstructions rely on extrapolation of available observations from continents, which introduces relatively larger uncertainties. Paleomagnetic data play a particularly important role in this context (e.g. Li et al., 2008, 2023; Pisarevsky et al., 2014; Kirscher et al., 2022; Meert and Santosh, 2022). However, in addition, the geological record preserved in the continents includes vast untapped information regarding the tectonic geography of the planet through time (Seton et al., 2023). Integrating these geological data with necessarily limited paleomagnetic information provides testable predictions for regions and time periods for which direct observations are lacking, especially when combined with empirically observed ‘rules’ of plate tectonics (e.g. Müller et al., 2022a). The resulting models, although still non-unique (e.g. with inferred plate boundaries and synthetic oceanic plates for pre-Pangean times), enable quantitative estimates of tectonic processes and provide insights into the connections between the deep Earth and its surface even with substantial uncertainties (Cao et al., 2021; Flament et al., 2022; Müller et al., 2022a).

The operation of plate tectonics during Mesoproterozoic times is debated. An interpretation of geological phenomena (e.g., high metamorphic thermobaric ratios) that suggest elevated mantle temperatures during this time (Brown et al., 2020; Tamblyn et al., 2021), has been related either to the insulation of a long-lived large supercontinent through much of the Mesoproterozoic (Gurnis, 1988; Tamblyn et al., 2021; Brown et al., 2022; Zou et al., 2023), or to a ‘single lid’ regime with limited lateral movement of plates (Stern, 2020). Roberts et al. (2022) argued for plate tectonics, albeit with different geodynamics (e.g. less or no deep continental subduction compared to the modern regime) due to higher temperatures from secular mantle cooling. They further suggested hot and wide continental back-arcs as the cause of Mesoproterozoic high temperature/pressure metamorphism and ‘dry’ ferroan magmatism (Roberts et al., 2023).

Despite the recent advances in modelling continental motions and plate boundary evolution, the construction of a continuous tectonic model, constrained by geological and high-quality paleomagnetic data and connecting the Phanerozoic and Mesoproterozoic, encompassing all three well-known supercontinents (Nuna, Rodinia, Pangea), has remained elusive. Li et al. (2023) introduced a paleomagnetic-focused reconstruction encompassing Nuna and Rodinia supercontinents. Here, we present a considerably different, new topological full-plate plate model spanning 1.8 Ga to the present day, through merging and updating previously published models and focusing particularly on the geological relationships between plates, as well as considering geophysical (e.g. paleomagnetic) constraints.

2. Methods

2.1 Model construction

Our 1.8 Ga–present full-plate reconstruction is built based on three published models (Fig. 1b) using GPlates (Müller et al., 2018). The model of Pisarevsky et al. (2014, referred to as P14) is the base model for times before 1.0 Ga, for which the model by Condie et al. (2021, referred to as C21) is also used. P14 and C21 are similar late Paleoproterozoic–Mesoproterozoic models with small differences: P14 has slightly smaller time intervals (~ 20–70 Myr) compared to C21 (100 Myr). Additionally, C21 covers a longer timespan (1800–1100 Ma) compared to P14 (1770–1270 Ma). For the period from 1.0 Ga to the present, we adopt the model from Merdith et al. (2021, referred to as M21), with minor adjustments made for the Neoproterozoic era. All three models are global plate models, with M21 extensively constrained by geological and geophysical data, and P14 and C21 constrained by paleomagnetic data and supplemented by geological data. P14 and C21 are "continental-drift" type models, lacking plate boundaries and oceanic plates, while M21 includes both continental blocks and a dynamic network of evolving plate boundaries.

The construction of our model involves the following steps. We first created a new model for the period 1800–1100 Ma by combining P14 and C21. Specifically, we used P14 for the time range of 1770–1270 Ma and employ C21 for the remaining time intervals. We subsequently linked this 1800–1100 Ma model to M21. To ensure a seamless transition, we introduce additional finite rotations based on available data for the period 1100–1000 Ma that is not covered by either base model. We then updated the model (e.g. improved the match of plates to paleomagnetic poles and adjusted the timings of collisions and rift events) by incorporating new paleomagnetic and geological data. Lastly, we constructed continuous plate boundaries, primarily focusing on the 1800–1000 Ma period.

We used the continental outlines from model M21 and make minor modifications to the continents that consisted of relatively small separate blocks before 1000 Ma (Fig. 1a). For example, Baltica is a single landmass in M21, but is divided into multiple small blocks in our model. Earth's surface before Nuna was likely comprised of numerous micro-continents (Li et al., 2018, 2023). The cratonic core of most continents formed during the amalgamation of Archean cratons along late Paleoproterozoic collisional zones (Zhao et al., 2002), with additional continental growth during Mesoproterozoic accretionary orogenies, such as those in Laurentia and Baltica (e.g. Whitmeyer and Karlstrom, 2007; Condie et al., 2021). Our pre-1.0 Ga reconstruction includes most major cratonic blocks (refer to Fig. 1 here and fig. 10 in Hasterok et al., 2022), with the exception of a few small blocks (e.g. the Rio de la Plata craton) due to limited data availability or insufficient evidence to confirm the existence of extensive pre-1.0 Ga basement. Consequently, these small blocks suddenly appear at 1.0 Ga. Some blocks also appear at 600 Ma in our model. We do not extend our model deeper in time than 1.8 Ga due to extensive continental fragmentation before this time (e.g. Lubnina et al., 2017; Zhao et al., 2002).

We then built a relative plate motion model similar to M21. The motions of all continents in P14 and C21 are constrained by paleomagnetic data and, therefore, are directly tied to the paleomagnetic reference frame. We recalculated the equivalent rotations of all blocks relative to an adjacent plate, incorporating them into a relative plate motion hierarchy while preserving their overall absolute motion. This conversion to a relative plate motion model is common when using geological data to model the relative motion of plates. It also facilitates future testing of alternative absolute reference frames, such as the no-net-lithospheric-rotation frame, by maintaining the relative plate motions. We highlight the utility of this approach as plate-tectonic phenomena responsible for lithospheric and earth-surface system evolution are controlled by plate interactions rather than their relationship to Earth's magnetic field.

During the existence of Rodinia, Laurentia is used as the base of the plate hierarchy in M21 due to its central position within the supercontinent. Although Laurentia was not located at the center of Nuna, we establish plate motion chains primarily tying most plates to Laurentia both for consistency and because it is the best-constrained continent for this time period. Laurentia is linked to Earth's spin axis through a paleomagnetic reference frame. The motions of plates within superoceans are tied to triple junctions, similar to the evolution of the Panthalassan plates in the Late Paleozoic (Young et al., 2019).

2.2 Paleomagnetic poles

Paleomagnetic data provide quantitative information about continental paleolatitudes and their azimuthal orientation. We compile 209 paleomagnetic poles with ages > 600 Ma (including 153 poles > 1000 Ma, Supplementary Data Table S1 and Fig. 2) from the GPMDB database (http://gpmdb.net; Pisarevsky et al., 2022), which is in turn based on previous studies (e.g. Pisarevsky et al., 2014; Evans et al., 2021). Supplementary Data Table S1 mostly contains poles with the quality factor of Van der Voo (1990) Q > 3. However, there are a few exceptions: nine poles with Q = 3 are included, shown in Supplementary Data Table S1 in italics. The reasons for these exceptions are: (i) the closeness of those poles to nearly coeval higher quality poles from the same continents (poles 407, 8848, 9367); (ii) an absence of any better poles for a long-time interval from some continents (poles 1962, 8275, 9135, 9165, 9277, 9520). While there are good data coverage for a few continents, including Laurentia, Baltica, North China, and North Australia, data are sparse or limited for some other continents. For example, there are no paleomagnetic poles for South China and Tarim older than 1.0 Ga, and there is only one such pole for West Africa. We use the poles to refine the base models or include continents that are not included in the based models.

Geological records are also used to constrain tectonic evolution. Tectonic phenomena, such as rifting/ocean formation, orogeny (accretionary or collisional), metamorphism and magmatism (e.g. arc volcanism), provide valuable insights into the relative motion of plates. The sedimentary record and detrital zircon peaks of similar age can also indicate potential plate affinities. Our model follows general plate tectonic rules or principles, e.g. there are three types of plate boundaries, and they are continuously connected; new crust forms at mid-ocean ridges and is recycled along subduction zones (Cox and Hart, 1991). Plate kinematic rules inferred from post-Pangea plate motions also serve as guides (Zahirovic et al., 2015), for instance, plates with over 50% continental fraction have root mean square (RMS) velocities < 10 cm/yr (while others may reach ~20 cm/yr); plates with any cratonic portion exhibit a median RMS velocity of ~5.8 cm/yr; global RMS speed generally falls between 4 and 10 cm/yr. We also attempt to smooth plate motion trajectories (fast changes are difficult to explain geodynamically) and make them as simple as possible.

There currently exists no widely accepted method to constrain the paleolongitude of plates. An approach has been suggested to reconstruct large igneous provinces (LIPs) and kimberlites, as well as the plates carrying them, to align with the edges of Large Low Shear Velocity Provinces (LLSVPs, Garnero and McNamara, 2008; Torsvik and Cocks, 2017). This approach assumes that the LLSVPs are fixed, and LIPs and kimberlites are the product of plumes rising along LLSVP edges (Burke et al., 2008; Torsvik et al., 2010). However, geodynamic models and seismic observations suggest that LLSVPs are deformable through interaction with cold slabs (Zhang et al., 2010; Frost and Rost, 2014; Flament et al., 2022). Furthermore, statistical analyses show that it cannot be distinguished whether the LIPs and kimberlites are correlated with LLSVP margins or with their interiors (Austermann et al., 2014; Davies et al., 2015). Mitchell et al. (2012) used paleomagnetic data to propose an “orthoversion” model (Evans, 2003) assuming pole paths are dominated by true polar wander (rather than tectonic motions), in contrast to previously proposed “introversion” and “extroversion” models (Murphy and Nance, 2003). In the "orthoversion" model, a new supercontinent assembles over the downwelling subduction girdle of the previous supercontinent, and two successive supercontinents are spatially ca. 90° away from each other. The longitudinal movements in our model are primarily derived from the base models, with minor adjustments made to reduce plate velocities and ensure a smoother transition to model M21. In our model, Nuna (based on P14) is about 105° away from Rodinia (derived mainly from M21), which is broadly compatible with "orthoversion".

2.3 Identification of plate boundary types

Metamorphic and geochemical data between 1850–800 Ma from Hasterok et al. (2022) are used to identify different tectonic environments (Fig. 3). Four thousand five hundred ages of igneous rocks, which are both I-type (derived from igneous protoliths) (Chappell and White, 1974), and magnesian-type (high magnesium to iron ratios) of FeO/(FeO+MgO) classification from Frost et al. (2001), are used to indicate potential subduction. Around 190 metamorphic gradients with age constraints have also been compiled (Brown and Johnson, 2018; Hasterok et al., 2022). High metamorphic gradients (> 775 K/GPa) are used to identify potential rifting (either in a back-arc setting or away from convergent plate margins), low metamorphic gradients (< 375 K/Gpa) indicate potential subduction and medium metamorphic gradients (between 375 K/Gpa and 775 K/Gpa) indicate potential orogenesis due to continental thickening. Other geological data are also used to build plate boundary zones: terrane accretion (Fig. 4, Supplementary Data Table S2) and arc/back-arc records are used to model subduction zones; mid-ocean ridges are built between continents with a history of rifting. Transform faults are primarily built to accommodate shearing plate motions or to link subduction zones and mid-ocean ridges. Modelled plate boundaries must also be consistent with paleomagnetic data (used to constrain continental motion). Different types of data are always combined to model plate boundaries.

Plate boundaries are more accurately constrained along continental margins with better-preserved geological records. Determining plate boundaries away from continents is challenging due to the lack of preserved ocean basins before the Mesozoic. In such cases, boundaries are inferred by connecting constrained boundaries or interpreting continental block motions. To maintain overall model consistency, some oceanic-only plates are introduced. For instance, a simple three-plate spreading scenario is implemented to ensure circum-Nuna subduction. These ridges and transforms are synthetic but with a reasonable spreading rate. Boundaries are iteratively constructed to ensure alignment with plate motion patterns and consistency with other boundaries. The lengths of mid-ocean ridges and subduction zones are inherently uncertain due to scarce data but remain valuable to test hypotheses about first-order global tectonic evolution.

3. Input models and modifications

P14 (the base model before 1 Ga) is based on a compilation of reliable paleomagnetic data (available before 2014) and is also constrained by geological observations. In P14, Nuna formed around 1650–1580 Ma by joining at least two stable continental landmasses formed by ca. 1.7 Ga: West Nuna and East Nuna. West Nuna includes Laurentia, Baltica and India. East Nuna includes North, West and South Australia, the Mawson craton of Antarctica and North China. Siberia and the

Congo/São Francisco craton were tentatively proposed as a third rigid continental entity that merged into Nuna at 1500 Ma. Amazonia-West Africa was located outside of Nuna. The breakup of Nuna occurred around 1460–1380 Ma, with East and West Nuna rifting apart.

M21 is a model spanning from 1 Ga to the present-day that combined several models for different time periods. At 1 Ga, M21 starts with most blocks (such as Laurentia, Baltica, Siberia, Amazonia, West Africa and some micro-blocks) being together. Australia, Mawson and North China were separated from these blocks by a transform boundary, and then joined Laurentia and other continents around 930 Ma to form Rodinia through dextral shearing. In this model, the breakup of Rodinia initiated at 800 Ma, resulting in the separation of Australia, Mawson, and North China from Laurentia and the opening of the Proto-Pacific Ocean (Merdith et al. 2017b). Subsequently, Gondwana had assembled by around 520 Ma.

The majority of the modifications we have made to the base models are to the late Paleoproterozoic–Mesoproterozoic eras (models P14 and C21, Fig. 5). Our refinements to M21 are limited to the Neoproterozoic era, as follows.

3.1. Nuna assembly and existence (1800–1460 Ma)

3.1.1 West Nuna (Laurentia, Baltica, South India, Yangtze)

Laurentia comprises several cratonic blocks, most of which amalgamated during 2.0–1.8 Ga orogenies (Hoffman, 2014; Swanson-Hysell, 2021). In particular, the ~1.86–1.82 Ga Trans-Hudson orogeny assembled the Slave/Rae/Hearne craton and the Superior craton, forming the major part of Laurentia (Swanson-Hysell, 2021). The Wyoming craton accreted onto Laurentia around 1.78–1.72 Ga, after the Big Sky orogeny (Harms et al., 2004), which is represented in our model at 1.75 Ga. The late Paleoproterozoic to Mesoproterozoic evolution of Laurentia is well constrained by paleomagnetic poles from P14 (Fig. 6). Our modifications to Laurentia are minor and include: (1) smoothing the motion of Laurentia to reduce fast plate movements (Fig. 7). In P14, Laurentia exhibited some zigzag motion (Fig. 7a), resulting in plate velocities up to 12 cm/yr between 1.5–1.4 Ga (Fig. 7b). The speed is reduced to ~2 cm/yr in our model. This adjustment is important as Laurentia is at the base of the plate hierarchy in our model, and its motion affects that of other plates. (2) Incorporating the accretion of small terranes along the present-day southeast margin of Laurentia, which were not accounted for in P14 (Fig. 6). This accretion mainly occurred during the 1.8–1.7 Ga Yavapai, the 1.7–1.6 Ga Mazatzal, and the 1.09–0.98 Ga Grenville orogenies (e.g. Karlstrom et al., 2001; Rivers, 2008). (3) Adjusting the plate positions to better align with paleomagnetic data (Supplementary Data Fig. S1).

We follow P14 and some other previous studies (e.g. Salminen and Pesonen, 2007), to juxtapose Baltica with Laurentia in Nuna, which is supported by paleomagnetic data and similar late Paleoproterozoic to Mesoproterozoic accretion records. Baltica consists of two parts: south-eastern Baltica (Sarmatia/Volgo-Uralia) and western Baltica (Fennoscandia), which assembled along the Central Russian Collision Belt during 1.8–1.7 Ga (Bogdanova et al., 2008). The collision was loosely constrained between 1720 Ma and 1650 Ma in P14, and 1700 Ma is adopted in our model.

In model P14, southern India is juxtaposed with south-eastern Baltica within Nuna (Fig. 5). This connection is supported by a paleomagnetic pole from the South Indian Block (the ~1466 Ma Lakhna dyke pole; No. 9408 in Supplementary Data Table S1), and based on the interpretation that the (present-day) southeastern India margin formed a Paleoproterozoic to Mesoproterozoic active margin in a similar manner to the (present-day) western Baltica margin (Dasgupta et al., 2013). The Indian Archean–Paleoproterozoic basement includes the South and North Indian Blocks separated by the Central Indian Tectonic Zone. The amalgamation of the two blocks was previously thought to have occurred during the Paleoproterozoic (e.g. Acharyya, 2003). Three metamorphic-magmatic events occurred along the Central Indian Tectonic Zone: a ca. 1.8–1.75 Ga event in the northern part and two later events, respectively, at ca. 1.62–1.54 Ga and ca. 1.06–0.94 Ga in the southern part (Bhowmik and Santosh, 2019; Chattopadhyay et al., 2020; Wang et al., 2021). The ca. 1.06–0.94 Ga event developed considerable crustal shortening and high-pressure metamorphism and is interpreted to mark the final collision between the North and South Indian blocks (Bhowmik et al., 2012; Bhowmik and Santosh, 2019). Therefore, we model the North and South Indian blocks as separated before this time. Our model considers the juxtaposition of only the South Indian Block with Baltica, as supported by paleomagnetic data, excluding the North Indian Block (Fig. 5).

The southern Eastern Ghats Belt adjacent to the eastern Dharwar Craton of the South Indian Block records ca. 1.90–1.60 Ga accretionary orogenesis, demonstrated by ultra-high temperature (UHT) metamorphism at ca. 1.76 Ga, the formation of magmatic arc at ca. 1.72–1.63 Ga, and subsequent collisional metamorphism at ca. 1.6 Ga (Dasgupta et al., 2013; Henderson et al., 2014). The Napier Complex of East Antarctica is interpreted as colliding with the Dharwar Craton at ~1.60 Ga (e.g. Harley, 2003; Henderson et al., 2014). The East Antarctic Rayner Province in M21 forms an along-strike extension of the northern Eastern Ghats Belt (Eastern Ghats Orogeny) at 1000 Ma, based on similar tectonic and metamorphic histories (Rickers et al., 2001; Dobmeier and Raith, 2003).

The Yangtze Block (western South China) lacks Paleo–Mesoproterozoic paleomagnetic data and is not included in P14. We model the Yangtze Block primarily based on a recent geological study (Cawood et al., 2020). Cawood et al. (2020) proposed that Hainan Island, now a part of Cathaysia Block (eastern South China), was a part of Yangtze Block during Proterozoic times, consistent with similarities in depositional ages and detrital zircon age spectra as well as Hf isotopic compositions of late Mesoproterozoic sedimentary units from southern Yangtze Block (Kunyang Group) and Hainan Island (Shilu Group) (Wang et al., 2012; Yao et al., 2017). Cawood et al. (2020) suggested that the Yangtze Block was situated offshore northern Laurentia, near northern Australia and southern Siberia in Nuna. This argument is supported by: (1) similar Archean–Paleoproterozoic tectonothermal histories for the Yangtze Block and NW Laurentia. Both regions underwent collision-related regional metamorphism around 2 Ga and subsequent extension-related A-type magmatism and metamorphism at ca. 1.85–1.80 Ga (Thorkelson et al., 2001; Wang et al., 2016; Cawood et al., 2020). (2) The detrital zircon signatures of late Paleoproterozoic–Mesoproterozoic sedimentary rocks in the Yangtze Block exhibit strong similarities with those from northwest Laurentia and northern Australia. For instance, the detrital zircon age distribution pattern of the late Paleoproterozoic upper

Dongchuan Formation matches well with the similar-aged Wernecke Supergroup in northwest Laurentia, the McArthur, Isa, and upper Etheridge successions in North Australia, and the Changcheng Group in North China (Wang and Zhou, 2014; Furlanetto et al., 2016). Similarly, the metasedimentary units in the Baoban Complex in Hainan (which was part of the Yangtze Block), with ages ranging from 1550 Ma to 1300 Ma, have similar detrital zircon age peaks with time equivalent units in western Laurentia (e.g. Belt Basin), northern Australia (Nordsvan et al., 2018; Yang et al., 2020). (3) The occurrence of similar Fe-Cu mineralization at ca. 1.6 Ga in southwestern Yangtze, northeast Australia, and northwest Laurentia (Thorkelson et al., 2001; Wang and Zhou, 2014). Recently, Zhao et al. (2023) proposed that the distinct basement ages between the northern and southwestern Yangtze are comparable to those of southern Siberia and northern Laurentia, respectively. Here, we model the Yangtze Block as between northern Laurentia and southern Siberia prior to Nuna breakup (Fig. 6).

3.1.2 East Nuna (Australia, East Antarctica, North China, North India, Cathaysia)

The modern Australian continent consists of three Archean to Paleoproterozoic blocks – the North Australian, West Australian and South Australian cratons. We follow P14 to keep proximity between North and South Australian cratons from 1.8 Ga (see Morrissey et al., 2023 for a recent review). The North Australian Craton underwent a southward motion by ~20° from 1800 Ma to 1760 Ma, as indicated by paleomagnetic data (Kirscher et al., 2019). The southern margin of the North Australian Craton formed a broad accretionary orogen from 1800 Ma to 1500 Ma, which is indicated in the model by the accretion of the Arunta Block at ca. 1740 Ma (representing most of the Aileron Province, Ahmad et al., 2013) and the Musgrave Block at ca. 1600 Ma (which consists of the Warumpi and Musgrave Provinces, Ahmad and Munson, 2013). The accretionary history is manifested by multiple orogenic events (e.g. the 1740–1690 Ma Strangways Orogeny, the 1640–1630 Ma Liebig Orogeny, and the 1600–1560 Ma Chewings Orogeny; Cawood and Korsch, 2008; Betts et al., 2011; Haines et al., 2016). In P14, the West Australian Craton was fixed to the North Australian Craton before Nuna assembly (Fig. 8). Instead, we model the West Australian Craton to be located near the Kalahari Craton at 1800 Ma. We suggest this proximity to reflect the shared history of the Pilbara and Kaapvaal cratons (i.e. Vaalbara, de Kock et al., 2009) until ca. 2.1 Ga, followed by the collision between the Pilbara and Yilgarn cratons to form the West Australian Craton represented by the 2005–1950 Ma Glenburgh Orogeny (Occhipinti et al., 2004; Johnson et al., 2011). The West Australian Craton drifted across an ocean (Fig. 8) and collided with the South Australian Craton at ca. 1380 Ma, resulting in the Albany-Fraser (Morrissey et al., 2017; Spaggiari et al., 2018), the Mount West (Howard et al., 2015) and the Parnngurr orogenies (Gardiner et al., 2018; Zhao et al., 2022).

We follow P14 in matching the western Laurentia margin with the northeastern North Australia margin and the eastern South Australia margin (Figs. 5, 6 and 8). This interpretation is based on paleomagnetic data and suggestions that eastern Australia-Antarctica provides 1600–1500 Ma zircon detritus for the lower Belt-Purcell Groups and correlatives (Ross et al., 1992; Goodge et al., 2017). We apply a slightly looser configuration than P14, considering that the blocks were likely larger than what is preserved. The collision between Australia–Antarctica and Laurentia, known as the Racklan Orogeny in Laurentia and the Isan Orogeny in Australia, has been recently constrained to ca. 1600 Ma based on geochronological studies (Nordsvan et al., 2018; Pourteau et al., 2018). Therefore, we update the collision time from 1650 Ma in P14 to 1600 Ma. The subduction polarity of the Australia-Laurentia convergence is controversial. The Wernicke Supergroup on the northern part of the western Laurentian margin exhibits a thickness that gradually increases towards the west, indicating a possible passive continental margin prior to the Racklan Orogeny (Mitchelmore and Cook, 1994; Thorkelson et al., 2005), even though it was also interpreted as a back-arc rifting margin (Nordsvan et al., 2018). The sedimentation age of the Wernicke Supergroup is debated, with studies proposing sedimentation before 1720 Ma (Thorkelson et al., 2005), or until later than 1640 Ma (Furlanetto et al., 2013). To the south of the Mackenzie Mountains, the Muskwa assemblage consists of unmetamorphosed siliciclastic and carbonate strata younger than ca. 1766 Ma based on the youngest detrital zircon (Ross et al., 2001). Seismic studies of these strata suggested a passive margin fabric (Cook et al., 2004). West dipping crust-penetrating thrusts in northeastern Australia (Korsch et al., 2012) fit the metamorphic record suggesting high-pressure ca. 1600 Ma metamorphism in the east forming a lower orogenic plate with the Mount Isa inlier forming an upper plate (Pourteau et al. 2018) whose sedimentary protoliths broadly correlate with coeval sedimentary rocks in the McArthur Basin (overlying the Northern Australian Craton) and are interpreted to be deposited within a basin to the continent side of a subduction zone (Rawlings, 1999; Betts et al., 2016; Nordsvan et al., 2018). Therefore, we model subduction dipping towards Australia.

P14 suggests a close proximity between North China and Australian blocks in Nuna, mainly based on 1.78–1.76 Ga and 1.46–1.41 Ga paleopoles from the two continents (Zhang et al., 2012). The similarity of Mesoproterozoic deposits (Cox et al., 2022), and the presence of ca. 1320 Ma LIPs in both northern North China and the McArthur Basin of northern Australia support their proximity (Zhang et al., 2012, 2017; Nixon et al., 2022). Recent paleomagnetic data also support the long-lived (~1.78 Ga to 1.32 Ga) connection between North China and North Australia (Wang et al., 2019). We maintain the North China-Australia connection but with slight adjustments. Instead of locating North China adjacent to the southwestern (present-day) North Australia, we position it next to the western margin, with subduction along the southern margin of North Australia (Fig. 8). The connection between North China and Australia is maintained during the period of 1000–650 Ma in model M21. Thus, we keep the two blocks next to each other between 1800 Ma and 650 Ma, and apply a small shift between them between 1236–1200 Ma to achieve a better fit with the paleomagnetic data. Overall, our updated configuration improves the match with paleomagnetic data (Supplementary Data Fig. S1) and simplifies the transition to the Rodinia configuration. The Mesoproterozoic Xiong'er Group in the southern North China Block consists of andesites and basaltic andesites formed at 1.78–1.75 Ga (He et al., 2009), with minor felsic volcanic rocks erupting at ca. 1.45 Ga, with lithological characteristics suggesting long-term subduction along the southern margin (Chen, 1992; Chen and Zhao, 1997; Zhao et al., 2003b). During this period, the northern margin of the North China Block experienced multi-stage intracontinental rifting (e.g. the Yanliao rift), and the deposition of thick clastic rocks and limestone between ca. 1.7–1.4 Ga (Li et al., 2019a).

The North Indian and South Indian blocks were recently suggested to have been separate in the Mesoproterozoic until amalgamation at ~1.0 Ga (see above). Based on similarities in Archean–Proterozoic metamorphic evolution, orogenesis and sedimentary-volcanic successions, North China and India were proposed to have been connected in Nuna, with the East and West blocks of North China connected to the South and North Indian blocks, respectively (Zhao et al., 2002). This configuration is adopted by many studies (Zhang et al., 2012; Li et al., 2019a). Pisarevsky et al. (2013) argued that a ca. 1466 Ma paleomagnetic pole from South India ruled out its position close to North China, and suggested a position next to Baltica. The location of North India is unconstrained. Here we tentatively leave the North Indian Block next to western North China prior to Nuna breakup and attach its northwest margin to the northern margin of North China (similar to fig.4 of Wang et al., 2021). As with many of the links proposed here, this positioning may need refinement as additional data becomes available.

The Cathaysia Block (eastern South China) is not included in P14 due to a lack of paleomagnetic data. Previous interpretations suggested a connection between Cathaysia and Southwest Laurentia in the Paleo-Mesoproterozoic, based on similarities between the 1430 Ma granites on Hainan Island (southwestern Cathaysia block) and similar-aged A-type granite province of Southwest Laurentia (Li et al., 2008; Yao et al., 2017). However, recent studies indicate that the Precambrian crustal components of Hainan Island are unrelated to Cathaysia but are instead linked to the Yangtze Block (Xu et al., 2016; Cawood et al., 2020; Wang et al., 2021). Recent proposals suggest a connection between the Cathaysia Block and the Lesser Himalaya of North India during the Proterozoic (Cawood et al., 2020; Wang et al., 2021), which is also adopted in model M21 for the Rodinia interval. High-grade metamorphism at 1.88–1.86 Ga in both the Cathaysia Block and Lesser Himalayan Block has been proposed to mark their collision (Richards et al., 2005; Yu et al., 2012). The collision was followed by synchronous (~1.83–1.80 Ga), within plate, mafic volcanism in the Aravalli-Delhi Fold Belt and Lesser Himalaya of the North India Block, and the Cathaysia Block (Liu et al., 2014; Miller et al., 2000; Wang et al., 2021). In addition, Paleoproterozoic sedimentary successions from both the North India Block (e.g. the Aravalli and Northern Delhi Supergroups; McQuarrie et al., 2008; Long et al., 2011) and Cathaysia Block (e.g. the Badu Complex; Yu et al., 2012) exhibit similar detrital zircon age peaks at ~2.5 Ga and ~1.85 Ga (Cawood et al., 2020; Wang et al., 2021). Therefore, we locate the Cathaysia Block adjacent to northern North Indian Block during the late Paleoproterozoic to Mesoproterozoic eras (Fig. 8).

3.1.3 South Nuna (Siberia, Tarim, Congo/São Francisco, Kalahari)

Siberia, which is nearly surrounded by Mesoproterozoic passive margins, is generally located in the interior of Nuna (Pisarevsky and Natapov, 2003; Evans and Mitchell, 2011). Many previous studies suggest Siberia existed off the northern Laurentia margin in Nuna, although different configurations have been proposed (Zhao et al., 2002; Pisarevsky et al., 2014; Ernst et al., 2016). Based on paleomagnetic data, P14 and related earlier studies (e.g. Pisarevsky et al., 2008) proposed that Siberia was located near the present-day northwest of Laurentia with a big ‘gap’ between 1500 Ma and 950 Ma. We accept the ‘gap’ proposal, but with adjustments to better match paleomagnetic poles (Supplementary Data Fig. S1). The fit of a paleomagnetic pole from southeast Siberia at 1730–1720 Ma (pole No. 9500 in Supplementary Data Table S1) with a ~1745–1736 Ma pole from Laurentia (pole 9139 in Supplementary Data Table S1) indicates a greater distance compared to those of 1475 Ma and 1050–950 Ma, suggesting that Siberia joined Laurentia-Baltica between 1740 Ma and 1475 Ma. Following recent suggestions of Cawood et al. (2020), Pisarevsky et al. (2021), and Zhao et al. (2023), we tentatively model Siberia accreting onto West Nuna at 1600 Ma with Yangtze placed between southern Siberia and northern Laurentia (Fig. 8).

Tarim was not included in P14 and most previous models due to limited geological studies and a lack of paleomagnetic data. Recent research on the northern Tarim margin has revealed a 1.94–1.91 Ga magmatic-metamorphic event occurred in an Andean-type continental arc, which was followed by collision at ca. 1.9–1.8 Ga (Ge et al., 2015). Similarly, collision-related granitic rocks of 2.0–1.8 Ga age are found in southern Siberia (Wang et al., 2020b). Detrital zircons from Proterozoic strata of northern Tarim and southern Siberia show a peak at 2.0–1.8 Ga and a lack of zircons between 1.7–1.1 Ga. Moreover, 2.0–1.8 Ga detrital zircons from the two continents show remarkably similar $\varepsilon_{Hf}(t)$ values. Consequently, Wang et al. (2020b) proposed that Tarim-Siberia were juxtaposed in Nuna after collision at 2.0–1.8 Ga. The Tarim-Siberia configuration is adopted in our model (Fig. 5).

In P14, the Congo/São Francisco craton is positioned directly south of Siberia, with São Francisco connected to the northern Siberia margin. Due to the lack of high-quality paleomagnetic poles, this argument is mainly based on coeval ca. 1500 Ma dyke swarms and ca. 1380 Ma magmatic events (Ernst et al., 2013). Here, based on ca. 1500 Ma palaeomagnetic poles from the two continents (poles 9552 and 9558), the Congo/São Francisco craton is rotated clockwise by 80° relative to Siberia compared to the P14 configuration, with southern Congo facing northern Siberia and also resulting in a larger distance between the two blocks (Fig. 5). At around 1790 Ma, we position the Congo/São Francisco craton to the east in the open ocean, with its latitude constrained by a paleomagnetic pole. We then employ a westward motion of the craton (Fig. 8), leading to its eventual joining with Siberia at 1650 Ma.

There are no reliable paleomagnetic data to constrain the location of Kalahari in Nuna. In P14, Kalahari forms the southernmost part of Nuna, surrounded by oceans, following Pesonen et al. (2003) and Jacobs et al. (2008). Recent studies suggest that dykes dated at ca. 1110 Ma in southern Congo may represent radial arms of the coeval Umkondo LIP in northern Kalahari as they have similar compositions, suggesting a possible connection between the two continents (Ernst et al., 2013; de Kock et al., 2014). Moreover, based on new paleomagnetic poles from the Kalahari dykes and the Umkondo LIP, Salminen et al. (2018) proposed a Kalahari-Congo configuration at 1110 Ma that is slightly different from that of the present-day. In this study, we adopt the Kalahari-Congo configuration proposed by Salminen et al. (2018) and extend it back to 1.8 Ga (Fig. 5).

3.1.4 Amazonia and West Africa

We leave West Africa-Amazonia separate from Nuna following P14 (Fig. 9). The hypothesis of Trompette (1994) that West Africa and Amazonia constituted a rigid continent resembling their Gondwanan configuration since the Mesoproterozoic has been widely accepted (e.g. Evans and Mitchell, 2011; Zhang et al., 2012). However, to match a recently published pole (No. 9968 in Supplementary Data Table S1) from West Africa at 860 Ma (Antonio et al., 2021), maintaining the Gondwanan configuration for the two blocks in Rodinia would require an anticlockwise rotation for them by ~80° relative to Laurentia, which is unreasonable. Here we keep the well-constrained Amazonia-Laurentia configuration in Rodinia, but introduce a new configuration for the Amazonia and West Africa based on the 860 Ma pole (Fig. 10). Other updates to P14 include: (1) making the southwestern margin of Amazonia, where subduction occurs, face the superocean most of the time (Fig. 9), and (2) applying four new poles. In our model, the Amazonia and West Africa continental blocks drifted in the ocean ~2000–5000 km west of Laurentia-Baltica from 1800 Ma until the assembly of Rodinia. We anticipate that this simple configuration will be improved as more data become available.

3.2. Nuna breakup and the initial assembly of Rodinia (1460–1000 Ma)

The breakup process of Nuna is not well described in the base models, as P14 ends at 1270 Ma, and C21 ends at 1100 Ma with ~100 Myr temporal resolution. We refine the base models for the period before 1100 Ma using available paleomagnetic poles and geological observations. For the 1100–1000 Ma period, we model the plates to obtain a smooth transition to M21.

During the late Mesoproterozoic, Baltica underwent a significant clockwise rotation by ~95° relative to Laurentia (Cawood et al., 2010). The exact timing of this rotation is uncertain. In C21, the separation between Baltica and Laurentia is modelled as beginning between 1300 Ma and 1200 Ma. Paleomagnetic data suggest that the clockwise rotation started after 1270 Ma and finished between 1050 Ma and 1000 Ma (Pisarevsky et al., 2003; Salminen and Pesonen, 2007; Pisarevsky and Bylund, 2010), coinciding with the collisional stages of the Grenville-Sveconorwegian orogeny (Bingen et al., 2008). Some studies propose that the clockwise rotation occurred between 1120 Ma and 1050 Ma (Evans, 2009; Salminen et al., 2009). This breakup is also proposed to be related to the 1270 Ma giant McKenzie magmatic event (Park, 1992) and the similar-aged Central Scandinavian Dolerite Complex (Elming and Mattsson, 2001). Structural evidence from Starmer (1996) suggests that the separation started around 1240 Ma. Considering these significant uncertainties, we model the clockwise rotation as occurring between 1235 Ma and 1020 Ma.

The timing of the breakup between South India and Baltica is poorly constrained because there is no evidence of Mesoproterozoic rifting in the western Dharwar Craton or the southwestern margin of Sarmatia (Pisarevsky et al., 2014). The breakup is not included in model P14 and starts between 1300 Ma and 1200 Ma in C21. However, P14 suggested a possible relation between the 1300–1100 Ma mafic sills in the western part of the Volyn-Orsha aulacogen (Bogdanova et al., 2008) and the Baltica-India rifting. They also proposed that the 1300–1100 Ma Volyn-Orsha aulacogen may represent a failed arm of a triple junction (Bogdanova et al., 1996) during the Baltica-India rifting. Additionally, a ca. 1190 Ma pole indicates South India was located at high latitudes, while Greenland (indicated by 1189–1179 Ma poles) and Baltica were at low latitudes, suggesting an earlier breakup timing. A breakup timing of 1270 Ma is adopted here.

The separation between Australia-Mawson and Laurentia is included in P14, which is largely adopted here (Fig. 11). According to P14, South Australia-Mawson rifted from Laurentia at ca. 1460 Ma, followed by the separation of North Australia at ca. 1380 Ma. This rift event marks the onset of Nuna breakup, which could be associated with the 1.38 Ga Hart River magmatism in northwest Laurentia, and subsequent deposition of the Pinguicula Group (Medig et al., 2009). This interpretation also agrees with a new ca. 1320 Ma pole from North Australia (pole No. 9978 in Supplementary Data Table S1)(Kirscher et al., 2021), which is consistent with Australia not far from Laurentia at this time. The sedimentary/provenance record of northern Australia (Yang et al., 2020, 2023) is interpreted to match the magmatic record of rifting in northern South Australia (Morrissey et al., 2019) to reflect a relatively early (ca. 1450 Ma) rifting between Australia and Laurentia. In model M21, dextral motion between Australia-Mawson and Laurentia during the late Stenian to early Tonian is proposed until the assembly of Rodinia at 930 Ma, based on correlation of 1.25–1.10 Ga strata in Tasmania and southwest Laurentia, and poles at 1.07 Ga and younger than 0.8 Ga (Mulder et al., 2018). This dextral motion model is also adopted here. In summary, in our model, Australia-Mawson rifts from Laurentia at 1460–1380 Ma, with spreading in the intervening ocean terminating at 1200 Ma. This episode of spreading is followed by a period of sinistral motion until 1070 Ma, followed by a resumption of dextral motion until the final assembly of Rodinia at 930 Ma, which is consistent with M21 and paleomagnetically viable. In our model, the North China and Australian blocks remain juxtaposed during the Nuna breakup process. In addition, we also model South China to begin rifting from Laurentia at 1380 Ma.

P14 proposed that Siberia could stay fixed to Laurentia with a gap (filled by the Yangtze Block in our model) between 1500 Ma and 950 Ma based on paleomagnetic poles. Even though the long-term relatively fixed Siberia and Laurentia configuration is feasible, we impose a small amount of rifting between the Siberia-Tarim and Laurentia-Baltica from 1235 Ma to 1200 Ma to achieve a better match with paleomagnetic poles during 1100–1000 Ma and 1500–1450 Ma. The onset of the rifting is modelled to occur simultaneously with the separation of Baltica from Laurentia, forming a triple junction between Siberia, Baltica and Laurentia (Fig. 11).

A ca. 1236 Ma paleomagnetic pole (pole No. 8123, Meert et al., 1994) indicates a significant distance between Congo/São Francisco and Laurentia at that time, suggesting an earlier breakup. We model the breakaway time of Congo/São Francisco at 1300 Ma, which aligns with the timeframe modelled in C21 (between 1300 Ma and 1200 Ma). During Nuna breakup, Kalahari remained attached to Congo/São Francisco, supported by poles at ca. 1110 Ma (Swanson-Hysell et al., 2015; Salminen et al., 2018). They are separated in Rodinia (as in M21), with Congo/São Francisco at high latitude at ca. 900 Ma and Kalahari at low latitude (Evans, 2013). The emplacement of the ca. 1110 Ga Umkondo LIP likely signifies the breakup of the Congo/São Francisco and Kalahari cratons (Salminen et al., 2018). We model the breakup at 1105 Ma, followed by separate accretions of the two blocks onto Rodinia.

Amazonia is traditionally positioned adjacent to Laurentia in Rodinia, with the 1300–1000 Ma Sunsas orogenic belt of southwest Amazonia (Litherland and Power, 1989; Santos et al., 2000) paired with the Grenville Orogen on the eastern margin of Laurentia (e.g. Hoffman, 1991; Pisarevsky and Natapov, 2003). Previous geological and paleomagnetic studies have suggested that Amazonia collided with the southern Grenville Province, followed by a ~3000 km sinistral strike-slip movement towards Baltica and northern Laurentia between 1200 Ma and 1000 Ma (Tohver et al., 2002, 2005a, 2005b). Evans (2013) proposed a clockwise rotation of Amazonia into Laurentia between ca. 1200 Ma and 1000 Ma, using the opposite polarities of the paleomagnetic poles and assuming a Mesoproterozoic Baltica-Amazonia connection. Apart from the poles used in previous studies, a new pole at 1110 Ma (Bispo-Santos et al., 2023) is used here. We consider a clockwise rotation of Amazonia between 1200 Ma and 1110 Ma, followed by an anticlockwise rotation until the final collision with Laurentia at 1070 Ma, documented by the ~1090–1020 Ma Ottawan orogenic phase (Rivers, 2015; Weller et al., 2021).

The Grenville, Sveconorwegian, and Sunsas orogens are traditionally viewed as having formed through continental collision between Laurentia and Baltica with Amazonia during Rodinia assembly (Li et al., 2008; Möller et al., 2013; Cawood and Pisarevsky, 2017), but some studies proposed that the Sveconorwegian orogen was an accretionary orogen, and Baltica was not a part of Rodinia (Slagstad et al., 2012, 2019, 2023). The paleomagnetic study of Kulakov et al. (2022), cited to support the separated Laurentia and Baltica at ~1090 Ma by Slagstad et al. (2023), was carried out on metamorphic rocks with imprecise ages of remanence and not supported by field tests. Coeval poles for Laurentia and Baltica are lacking between 1000–650 Ma, with the ones at ~615 Ma supporting their juxtaposition (before the opening of the Iapetus Ocean at 600 Ma). Here we adopt the traditional "collisional" Sveconorwegian orogen model and contiguous Baltica–Laurentia-Amazonia in Rodinia, while acknowledging the potential need for future refinements.

Laurentia and continents around it (e.g. Baltica, Siberia, and Australian blocks) experienced fast coherent southward motion between 1110 Ma and 1070 Ma, with speeds exceeding 20 cm/yr during ~1110–1100 Ma (Swanson-Hysell et al., 2019) and generally below 15 cm/yr the rest of the time. This coherent fast motion potentially involves both true polar wander and tectonic motion (Swanson-Hysell et al., 2019). More paleomagnetic poles from continents other than Laurentia are necessary to better constrain and understand this motion.

3.3 Rodinia final assembly and post-Rodinia (1000 Ma–present)

We have made minor modifications to M21 based on new data. One important change is to the evolution of West Africa, which underwent rifting from Amazonia during the breakup of Rodinia and subsequently accreted onto the Sahara Metacraton to form the African continent (Fig. 12). This alteration is partly because the West Africa-Amazonia configuration is changed here based on an 860 Ma pole (Fig. 10). We adjust the rift timing from 850 Ma in M21 to 720 Ma in our model based on the observation that rocks of the middle Neoproterozoic Assabet el Hassiane Group (Mauretanian Taoudeni Basin) are interpreted to be deposited within active rift basins (Bradley et al., 2022). We still follow M21 in modelling the accretion onto the Sahara Metacraton at 600 Ma.

In addition, the breakup time between Australia and Laurentia is changed from 800 Ma in M21 to 780 Ma in our model. Previous geological and paleomagnetic data poorly constrained the rifting and transition from rift-to-drift between Australia and Laurentia between 825 Ma and 700 Ma (e.g. Merdith et al., 2017a). While M21 adopted an early rifting at 800 Ma to achieve a low relative spreading velocity, they acknowledged that a later rifting before 770 Ma is kinematically feasible. Recently improved chronostratigraphic constraints from western Laurentia indicate that the rifting started at ~ 780 Ma (Macdonald et al., 2023). Here we follow Macdonald et al. (2023) to update the breakup timing to 780 Ma, which also leads to a slightly better fit to a new 775 Ma pole (No. 9975 in Supplementary Data Table S1) from North China.

We make slight adjustments to the positions of South China and India to better match an 802 Ma pole from South China (No. 9117 in Supplementary Data Table S1). Following M21, we maintain the connection between South China and India during the late Mesoproterozoic and Neoproterozoic eras based on their comparable Tonian accretionary histories. In addition, we have made other minor alterations, including slightly adjusting the relative positions of North China and North Australia to avoid overlap and adjusting the position of Siberia to better match paleomagnetic data between 1050 Ma and 950 Ma.

4. Global plate model between 1.8 Ga and 1.0 Ga

The base models provide detailed descriptions of the global reconstructions, and our updates to them are outlined in Section 3. In this section, we summarize the major tectonic events between 1.8 Ga and 1.0 Ga, which are the focus of our refinements in this study.

Our model starts with a quasi-supercontinent at 1.8 Ga (Fig. 13 and Supplementary Data Fig. S2), with most continents in geographical proximity at low latitudes. At 1.7 Ga, the collision between Sarmatia/Volgo-Uralia and Fennoscandia resulted in the formation of Baltica. Concurrently, South India joined Baltica and Laurentia, forming the West Nuna continent. To the east, the Australia blocks, Mawson, North China, North India, and Cathaysia formed East Nuna. East and West Nuna were separated by a narrow ocean at 1.8 Ga. Siberia had not joined Laurentia at this point, constrained by a pole at ca. 1.72 Ga. Congo/São Francisco and Kalahari moved westward from the open ocean and joined Siberia at 1.65 Ga to form South Nuna. Eventually, the East, West, and South Nuna merged at 1.6 Ga, causing the Racklan/Isan orogeny (e.g. Pourteau et al., 2018; Volante et al., 2020).

After assembly, Nuna was centered at the equator and exhibited very slow anticlockwise motion before its eventual breakup. This rotation was interpreted as true polar wander by Li et al. (2013). In the opposite hemisphere, the superocean was occupied by three large oceanic plates. Nuna’s exterior margin experienced long-term accretionary orogenesis (Condie, 2013; Roberts, 2013; Johansson et al., 2022; Roberts et al., 2022) that is found preserved along the margins of eastern Laurentia, southwestern Baltica, eastern Dharwar, southern North China, and southern North Australia (Fig. 4). Note that rather than the proposed Proterozoic single-lid hypothesis of Stern (2020), this extensive subduction/accretion orogenesis reflects Phanerozoic-like plate tectonics in the presence of a major supercontinent (Roberts et al., 2022).

The breakup of Nuna primarily occurred between ca. 1.46–1.3 Ga, initiating from the north and progressing towards the south. At 1.46 Ma, Mawson and South Australia began to rift away from Nuna. This rifting was followed by the separation of North Australia, Yangtze, North India, and Cathaysia at 1.38 Ga. West Australia collided South Australia and North Australia at 1.38 Ga, suggesting that it was never a part of Nuna. At 1.3 Ga, Congo/São Francisco and Kalahari separated from the supercontinent, with Congo shifting from 30°S to an equatorial region by 1.24 Ga. South India broke away from Baltica at 1.27 Ga and moved towards the polar area. The breakup of Nuna was accompanied by the extensive formation of LIPs throughout the interior of Nuna during 1.4–1.3 Ga (Li et al., 2019a; Condie et al., 2021; Zhang et al., 2022). Examples include the 1.38 Ga Hart River–Salmon River Arch LIP in western Laurentia (Doughty and Chamberlain, 1996), the 1.38 Ga Midsommersø–Zig-Zag Dal LIP in eastern North Greenland (Upton et al., 2005), the 1.32 Ga Yanliao LIP in North China (Zhang et al., 2017), and the 1.32 Ga Derim Derim-Galiwinku LIP in North Australia (Nixon et al., 2022).

Baltica experienced a ~95° clockwise rotation relative to Laurentia between 1235 Ma and 1020 Ma, and remained adjacent to Laurentia in the Rodinia supercontinent (Cawood et al., 2010). Congo/São Francisco and Kalahari moved eastward across the ocean and reached their westernmost position in Rodinia as depicted in M21. We try to model the movement of these blocks along the shortest path. North India and the Cathaysia Block remained connected during the breakup of Nuna and the assembly of Rodinia. Yangtze accreted onto Cathaysia to form South China around 900 Ma following M21 (though a collision age of ~830–800 Ma has also been proposed; e.g., Yao et al., 2019; Park et al., 2021). Around 980 Ma, South India accreted onto North India to form Neoproterozoic India (Collins and Pisarevsky, 2005). South China and India remained outside of Rodinia according to M21. After the breakup of Nuna, the Australian blocks and North China gradually drifted away from Laurentia until 1200 Ma. Subsequently, they underwent left-lateral transform movement relative to Laurentia, followed by right-lateral shear after 1070 Ma. They ultimately rejoined Laurentia at 930 Ma, marking the final formation of Rodinia (but see also Ding et al., 2021).

In our model, West Africa and Amazonia stayed in the ocean to the west of Nuna from 1800 Ma until their collision with Laurentia at 1070 Ma. The positions of the two blocks during this period are constrained by nine paleomagnetic poles (one pole from West Africa, and eight from Amazonia).

5. Model analysis and discussion

We quantify and evaluate the model in terms of the match to paleomagnetic data (Fig. 14), the lengths of ridge and trench, and associated plate motion rate through time (Fig. 15). We calculate the misfit between our model and the paleomagnetic poles, which is defined as the minimum great circle distance between the North Pole and the reconstructed paleomagnetic pole within the valid time range (Merdith et al., 2021). The mean misfit for all plates is about 12° (Fig. 14 and Supplementary Data Fig. S1), which is smaller than the 19° misfit for P14. The large misfit of P14 is partly due to the fact that some of the poles were published after the development of that model.

The modelled total length of ridges and transforms for 1.8–1.0 Ga is considerably shorter than that of present-day (but is not very different from that of the Paleozoic). The short length of ridges is likely because: (1) we only model major cratonic blocks in the Proterozoic, which produce less ridges when continents breakup, and (2) we build simple three-ridge configurations for major oceans, which contrasts with the modern Pacific Ocean, which is characterized by a larger number of plates, and therefore long ridges and transforms. The length of mid-ocean ridges is low during times of supercontinent existence and high during times of supercontinent breakup as new ridges are modelled in newly created interior oceans. The length of plate boundary also depends on interpretations of geological data. For example, placing Amazonia in the ocean prior to Rodinia assembly could lead to slightly longer mid-ocean ridges and subduction zones than placing Amazonia next to Baltica (the SAMBA connection, Johansson, 2009) during the same period. The global subduction zone length does not exhibit cyclical changes with the supercontinent cycle as the length of ridges does. Subduction zones are primarily identified based on accretion events, magmatic, and metamorphic records (Figs. 3 and 4). In some cases, they are interpreted from the sedimentary record or extrapolated due to limited rock exposure. For instance, in Cathaysia, the exposed pre-Neoproterozoic rocks are late Paleoproterozoic granitoids (~1910–1780 Ma) (Cawood et al., 2020), with Mesoproterozoic rocks rarely exposed. Thus, subduction is inferred during the late Paleoproterozoic and assumed to continue into the Mesoproterozoic (Figs. 8 and 11). Similarly, in eastern São Francisco, the Mesoproterozoic Espinhaço sequences (including marine deposits) document rifting and magmatism (Alkmim and Martins-Neto, 2012), suggesting possible back-arc rifting during this period. Thus, subduction is modelled in this region during this time (Figs. 8 and 11). Therefore, the modelled plate boundary length is uncertain due to limited preserved data (especially the loss of seafloor), and here only represents a first-order estimate.

The RMS speeds of all plates for most of the time before 1.0 Ga are between 4 and 7 cm/yr, consistent with those of post-Pangean times. However, the RMS speed exceeds 15 cm/yr at 1110–1100 Ma, due to the rapid coherent southward motion of Laurentia and adjacent continents (e.g. Baltica and Siberia), potentially involving both true polar wander and tectonic motion (Swanson-Hysell et al., 2019). While Laurentia's motion is well constrained by paleomagnetic poles, additional poles from other continents are necessary to further constrain this process. The RMS speeds tend to be low when supercontinents exist and high during supercontinent breakup, reflecting the relatively stability of large landmasses (Zahirovic et al., 2015). The net lithospheric rotation is generally below 0.2°/Myr between 1.8 Ga and 1.3 Ga, which is lower than the upper limit of 0.26°/Myr constrained by global azimuthal anisotropy (Conrad and Behn, 2010). However, the net rotation is much larger between 1.3 Ga and 1.0 Ga, peaking at ~1.4°/Myr around 1.1 Ga (due to the fast motion of Laurentia and neighboring plates). These large values also partly reflect the relatively fast absolute motion of plates while continents are widely dispersed. The global RMS speeds through time show similar trends to net lithospheric rotations, indicating that changes in plate speed are partly caused by net rotations. The RMS speeds are expected to be smaller and exhibit less variability over time when net rotations are reduced to below 0.2°/Myr (Müller et al., 2022a).

Attempts to reconstruct Nuna have progressed considerably in the last two decades, from earliest individual snapshots of continental configurations (Zhao et al., 2002), to quantitative kinematic modelling of continents (Pisarevsky et al., 2014), and models with both continental motion and evolving tectonic boundaries (Li et al., 2023, and our new model). Regarding the configuration of Nuna, the positions of some blocks are largely agreed on (Evans, 2013). For instance, the Laurentia-Baltica connection is well constrained by paleomagnetic poles and geological links, with Siberia situated next to the present-day northern Laurentia either with a 'gap' (P14; Pisarevsky et al., 2021 and here with a 'gap' filled by Yangtze) or not (Evans and Mitchell, 2011; Evans et al., 2016; Pehrsson et al., 2016; Li et al., 2023), Australia-Mawson is located near present-day western Laurentia. However, other blocks, such as West Africa-Amazonia, India and South China, are more disputed, and their locations in our reconstruction are different from those of some other models (e.g. Li et al., 2023).

The western margin of Amazonia was an accretionary boundary during the Paleoproterozoic–Mesoproterozoic (Cordani et al., 2009 and references therein) similar to Baltica, which led previous workers to propose a long-term 1800–900 Ma Amazonia-Baltica connection (SAMBA reconstruction, Johansson, 2009; Johansson et al., 2022). However, Fuck et al. (2008) pointed out that the late Paleoproterozoic Ventuari-Tapajós and Rio Negro-Juruena accretionary provinces are truncated by the younger Late Mesoproterozoic orogen in their northern parts, which questions the connectivity of the accretionary belts in Baltica and Amazonia. Moreover, the Putumayo orogeny (Ibañez–Mejia, 2020 and references therein) implies the presence of ocean northwest of Amazonia (in present-day coordinates) since at least 1.45 Ga until its 1.0–0.95 Ga collision with Baltica. P14 argued that the SAMBA reconstruction is not in good agreement with paleomagnetic data. The detailed geochronological study of the Svecofennian orogen in Baltica shows the direction of tectonic transport nearly orthogonal to that in the Ventuari-Topajos orogeny in Amazonia, which suggested to be a continuation of the former in the SAMBA model (see fig. 9 in Bogdanova et al., 2015). Li et al. (2023) keep Amazonia and Baltica next to each other in both Nuna and Rodinia, but with different configurations. Here, we follow P14 to leave Amazonia out of Nuna, but we recognize that more studies are required to settle this debate.

The hypothesized position of India within Nuna varied considerably in previous studies. It has been tentatively placed near North China (Zhao et al., 2002; Zhang et al., 2012; Li et al., 2019a), adjacent to Sarmatia (southeastern Baltica) in P14, or offboard present-day southern Laurentia (Li et al., 2023). Recent studies have constrained the amalgamation of North and South India to ca. 1.0 Ga (Bhowmik and Santosh, 2019), which means they need to be considered separately for the Paleoproterozoic and Mesoproterozoic. We combine these models and locate South India next to Sarmatia based on paleomagnetic data and similar accretion history, and North India next to North China.

The locations of Yangtze and Cathaysia (blocks of South China) during the time of Rodinia and Nuna are also controversial (Zhao et al., 2002; Li et al., 2008; Merdith et al., 2017a; Cawood et al., 2020). Some models ('missing-link' model) suggest an internal location of South China within Rodinia, placing it between Laurentia and Australia-Mawson (e.g. Li et al., 2008, 2023; Yao et al., 2017). The ca. 1430 Ma granites found on Hainan Island have been correlated with similar granites in western Laurentia, leading to the argument that Cathaysia was located next to present-day western Laurentia within Nuna (e.g. Yao et al., 2017; Li et al., 2023). In Li et al. (2023), Yangtze is located offboard southern Laurentia in Nuna, and subsequently experienced a dextral motion until accretion with Cathaysia-Laurentia at ca. 900 Ma. To move South China to their outboard positions in Gondwana, these 'missing-link' models involve unrealistically-large plate velocities and Euler-pole switches unseen in the Phanerozoic (Merdith et al., 2017b). Other models favor either a peripheral location for South China in Rodinia, or separation from Rodinia (e.g. M21). These models argue that Cathaysia was connected to northern India from at least the Paleoproterozoic, based on similarities in the age distribution of rock units (e.g. Merdith et al., 2017a; Yu et al., 2009). We also note that it is uncertain whether Hainan Island was even part of Cathaysia. Cawood et al. (2020), Pisarevsky et al. (2021) and Zhao et al. (2023) argued that Hainan formed a part of Yangtze before the Paleozoic, and that Yangtze was between northern Laurentia and southern Siberia in Nuna. Here, we adopt the latter scenario in alignment with M21.

There are many other debated or unresolved issues regarding the evolution of the Proterozoic plates. For instance, the exact configuration of Nuna and Rodinia and how many cratons were independently drifting outside of them are still disputed. The assembly timing of Nuna was initially proposed at ca. 1.8 Ga based on global-scale orogeny (Zhao et al., 2002), and this timing has been accepted by many studies (e.g. Zhang et al., 2012; Li et al., 2019a). Recent studies proposed later assembly at 1.65 Ga (Elming et al., 2021), ~1.6 Ga (Pourteau et al., 2018), or ~1.55 Ga (Pehrsson et al., 2016). In our model, most continents were in close proximity at 1.8 Ga, while the final assembly of Nuna occurred at 1.6 Ga, following recent geochronological studies of Racklan/Isan orogeny (Pourteau et al., 2018; Volante et al., 2020). The breakup timing of Nuna was argued during 1.5–1.25 Ga (Evans and Mitchell, 2011), around 1.35 Ga (Pehrsson et al., 2016), or soon after ca.1.3 Ga based on paleomagnetic poles (Kirscher et al., 2020; Li et al., 2023). Here we model the breakup initially starting at 1460 Ma, with the main breakup phase occurring at ca. 1380 Ma when East Nuna drifted away, which matches well with LIPs records in western Laurentia and East Nuna (e.g. Condie et al., 2021). Regarding the duration of Nuna, it is estimated to be ~300 Myr in Li et al. (2023), and ~200 Myr in Pehrsson et al. (2016). In our model, Nuna existed for 160 Myr, which is slightly longer than the durations of 150 Myr for Rodinia and 120 Myr for Pangea.

As the two only topological plate models covering both Nuna and Rodinia, the discussion above shows many differences between our model and the one presented in Li et al. (2023), for instance, the locations of South China, Amazonia-West Africa, and India during the Nuna and Rodinia intervals. We suggest that many of these differences are partly due to our model placing more emphasis on geological data compared to Li et al. (2023). Despite these discrepancies, the two Proterozoic models cover different possibilities, which can be beneficial for conducting uncertainty analysis in future studies (e.g. geodynamic modelling). The two models are both presented in a paleomagnetic reference frame, implying that the modelled plate motions may incorporate some degree of true polar wander. For example, the gradual counterclockwise rotation of Nuna is attributed to true polar wander by Li et al. (2023). In order to use the plate model in a geodynamic context in future, it is necessary to establish a mantle reference frame that is free of true polar wander.

Based on similarities between Nuna and Rodinia (e.g., similar Australia/Mawson-Laurentia and Laurentia-Siberia-Baltica connections), it is suggested that Nuna experienced an incomplete breakup, followed by assembly of Rodinia by introversion (e.g. Li et al., 2019b). Supercontinent assembly generally involves both introversion and extroversion; for example, Gondwana formed by extroversion from Rodinia, subsequently colliding with Laurentia to form Pangea by introversion (Hoffman, 1991; Murphy and Nance, 2003). Evans (2021) proposed that the Grenvillian-Sveconorwegian-Sunsas subduction/orogeny occurred along southeastern (present-day) Laurentia was an extroverted process, slightly preceding but overlapping in time with an introverted phase between western Laurentia and Australia-Mawson-North China. Our model suggests that Nuna did not fully break up, similar to Li et al. (2023), with Australian, Mawson, and North China blocks remaining together during the breakup, while Baltica and Siberia only adjusted slightly relative to Laurentia. Our model suggests a Nuna-Rodinia transition style similar to Evans (2021), with an extroverted evolution along the southeastern margin of Laurentia, and a slightly later introverted phase along the western margin. Wang et al. (2020a) proposed a dual megacontinent-supercontinent cycle, wherein the assembly of supercontinents was each preceded by ~ 200 Myr by the amalgamation of a megacontinent. Our model does not exactly show this dual cycle, but it does show small continents initially converging to form two to three large continents, which subsequently amalgamate into a supercontinent. For example, Nuna involves the convergence of three major continents (East, West, and South Nuna), while the assembly of Rodinia involves the initial joining of Laurentia-Baltica-Amazonia-West Africa, followed by their amalgamation with Australia-Mawson-North China to form the supercontinent.

We present this model as our best attempt at matching the voluminous geological and geophysical data that exists in this context. Contrary to the concept of a "boring billion" (c.f. Holland, 2006), our model reveals a dynamic geological history between 1.8 Ga and 0.8 Ga, which is characterized by supercontinent assembly and breakup, continuous accretion events, and widespread LIP events. We recognize and promote that our model is imperfect (for instance continents sometimes rotate around a proximal pole, mostly because they are modelled to match multiple paleomagnetic poles) and that any part of the model can/should be queried and improved on using more information, more data, and a better understanding of existing data. As such, this model is a snapshot and a means of presenting and focusing geological questions. We argue that our methodology of focusing on plate interactions and, therefore using the wealth of geological information preserved on the continents, is more robust than approaching the problem solely using paleomagnetic data, which are still too scarce to produce unambiguous Precambrian paleogeographic reconstructions in isolation. Ultimately, there is a solution that incorporates all data and we encourage researchers to modify and improve our model. Despite all the caveats required when presenting the results of this ambitious study, we suggest that our model is constrained by considerable data, and that it captures the first-order plate evolution for the last 1.8 billion years. We also keep the plate configurations simple in our model, so that it can be easily refined as additional data become available.

6. Conclusions

We present a new full-plate tectonic reconstruction, with evolving plate boundaries, from 1.8 Ga to present, building on previously published models. We smooth the motion of major plates in the base models to remove unreasonably fast motions, and to improve the match to paleomagnetic poles. The plate boundaries and plate interactions are constrained by magmatic, metamorphic, geochronological and sedimentary data that are interpreted in a tectonic geographic framework to be able to inform the reconstruction. In our model, Nuna formed at 1.6 Ga through the assembly of three landmasses: West Nuna, East Nuna and South Nuna. The North and South Indian blocks are considered separately, with South India juxtaposed southern Baltica, and North India next to North China. Yangtze is located between northern Laurentia and southern Siberia, and Cathaysia is connected to North India. Amazonia, West Africa and West Australia were not part of Nuna. Nuna then broke up mainly between 1.4–1.3 Ga, initially at the north, and propagating towards the south. The breakup timing matches LIPs records. Separated continents came together again to form Rodinia around 930 Ma, which later fragmented at ca. 780 Ma. Our model spans three supercontinents and more than two supercontinent cycles. We have produced a new tectonic framework for analyzing the long-term evolution of Earth systems, providing a basis for developing future analysis of tectonic controls on deep Earth resources and developing planetary hypsographic reconstructions that can inform lithosphere/earth surface systems feedbacks.

Acknowledgements

XC is supported by Shandong Outstanding Youth Science Foundation (China) (2023HWYQ-065), Taishan Scholar Program (China) (tsqn202306114) and National Key R&D Program of China (2022YFF0800401). ASC acknowledges funding through Australian Research Council projects LP210200822, LP200301457, FT120100340, FL240100114 and the MinEx CRC. His contribution forms MinEx publication #2024/37. SL is funded by National Natural Science Foundation of China (Nos. 42121005, 91958214), Shandong Provincial Natural Science Foundation (China) (No. ZR2021YQ25), and the Marine S&T Fund of Shandong Province for Pilot National Laboratory for Marine Science and Technology (Qingdao, China) (No. 2022QNLM050302). SP was supported by the Australian Research Council Laureate Fellowship grant to Z.X. Li (FL150100133). This study is a contribution to IGCP 648. NF acknowledges funding through Australian Research Council projects LP220100056 and FT230100001. Three anonymous reviewers are thanked for their constructive reviews that substantially improved the manuscript.

CRediT authorship contribution statement

XC: Methodology, Investigation, Visualization, Writing – Original Draft. ASC: Investigation, Writing – Review & Editing. SP: Methodology, Investigation, Writing - Review & Editing. NF: Conceptualization, Investigation, Writing – Review & Editing, Supervision. SL: Investigation, Writing – Review & Editing, Supervision, Funding acquisition. DH: Methodology, Investigation, Writing – Review & Editing. RDM: Conceptualization, Writing – Review & Editing, Resources, Supervision.

Data availability

The model is available on Zenodo at: https://doi.org/10.5281/zenodo.11536686.

Declaration of interests

The authors declare that they have no known competing financial interests or personal relationships that could have appeared to influence the work reported in this paper. Sanzhong Li is a Council Member of Geoscience Frontiers and the co-author of this article. This article was handled without any involvement of Sanzhong Li.

References

Acharyya, S., 2003. The nature of Mesoproterozoic Central Indian Tectonic Zone with exhumed and reworked older granulites. Gondwana Res. 6(2), 197-214.

Ahmad, M., Scrimgeour, I., Munson, T., 2013. Geological framework. Geology and Mineral Resources of the Northern Territory. Northern Territory Geological Survey, Special Publication, 5, 1-16.

Alkmim, F.F., Martins-Neto, M.A., 2012. Proterozoic first-order sedimentary sequences of the São Francisco craton, eastern Brazil. Mar. Pet. Geol. 33(1), 127-139.

Antonio, P.Y.J., Baratoux, L., Trindade, R.I.F., Rousse, S., Ayite, A., Lana, C., Macouin, M., Adu, E.W.K., Sanchez, C., Silva, M.A.L., Firmin, A.-S., Martínez Dopico, C.I., Proietti, A., Amponsah, P.O., Sakyi, P.A., 2021. West Africa in Rodinia: High quality paleomagnetic pole from the ~860 Ma Manso dyke swarm (Ghana). Gondwana Res. 94, 28-43.

Austermann, J., Kaye, B.T., Mitrovica, J.X., Huybers, P., 2014. A statistical analysis of the correlation between large igneous provinces and lower mantle seismic structure. Geophys. J. Int. 197(1), 1-9.

Betts, P.G., Armit, R.J., Stewart, J., Aitken, A.R.A., Ailleres, L., Donchak, P., Hutton, L., Withnall, I., Giles, D., 2016. Australia and Nuna. Geol. Soc. London Spec. Pub. 424(1), 47-81.

Betts, P.G., Giles, D., Aitken, A., 2011. Palaeoproterozoic accretion processes of Australia and comparisons with Laurentia. Int. Geol. Rev. 53(11-12), 1357-1376.

Bhowmik, S.K., Santosh, M., 2019. The current status of orogenesis in the Central Indian Tectonic Zone: A view from its Southern Margin. Geol. J. 54(5), 2912-2934.

Bhowmik, S.K., Wilde, S.A., Bhandari, A., Pal, T., Pant, N.C., 2012. Growth of the Greater Indian Landmass and its assembly in Rodinia: Geochronological evidence from the Central Indian Tectonic Zone. Gondwana Res. 22(1), 54-72.

Bingen, B., Nordgulen, O., Viola, G., 2008. A four-phase model for the Sveconorwegian orogeny, SW Scandinavia. Norsk Geol. Tidsskr. 88(1), 43.

Bispo-Santos, F., D'Agrella-Filho, M.S., de Almeida, R.P., Ruiz, A.S., Patroni, O.A., Silva, J.M., 2023. Paleomagnetic study of the 1112 Ma Huanchaca mafic sills (SW Amazonian Craton, Brazil) and the paleogeographic implications for Rodinia supercontinent. Precambrian Res. 388, 107013.

Bogdanova, S., Gorbatschev, R., Skridlaite, G., Soesoo, A., Taran, L., Kurlovich, D., 2015. Trans-Baltic Palaeoproterozoic correlations towards the reconstruction of supercontinent Columbia/Nuna. Precambrian Res. 259, 5-33.

Bogdanova, S., Pashkevich, I., Gorbatschev, R., Orlyuk, M., 1996. Riphean rifting and major Palaeoproterozoic crustal boundaries in the basement of the East European Craton: geology and geophysics. Tectonophysics 268(1-4), 1-21.

Bogdanova, S.V., Bingen, B., Gorbatschev, R., Kheraskova, T.N., Kozlov, V.I., Puchkov, V.N., Volozh, Y.A., 2008. The East European Craton (Baltica) before and during the assembly of Rodinia. Precambrian Res. 160(1-2), 23-45.

Bradley, D.C., Evans, D.A., O'sullivan, P., Taylor, C.D., Eglington, B.M., 2022. The Assabet barcode: Mesoproterozoic detrital zircons in Neoproterozoic strata from Mauritania, West Africa. Am. J. Sci. 322(8), 939-992.

Brocks, J.J., Jarrett, A.J.M., Sirantoine, E., Hallmann, C., Hoshino, Y., Liyanage, T., 2017. The rise of algae in Cryogenian oceans and the emergence of animals. Nature 548(7669), 578-581.

Brown, M., Johnson, T., 2018. Secular change in metamorphism and the onset of global plate tectonics. Am. Mineral. 103(2), 181-196.

Brown, M., Johnson, T., Spencer, C.J., 2022. Secular changes in metamorphism and metamorphic cooling rates track the evolving plate-tectonic regime on Earth. J. Geol. Soc. 179(5), jgs2022-050.

Brown, M., Kirkland, C., Johnson, T., 2020. Evolution of geodynamics since the Archean: Significant change at the dawn of the Phanerozoic. Geology 48(5), 488-492.

Burke, K., Steinberger, B., Torsvik, T.H., Smethurst, M.A., 2008. Plume Generation Zones at the margins of Large Low Shear Velocity Provinces on the core–mantle boundary. Earth Planet. Sci. Lett. 265(1-2), 49-60.

Cao, X., Flament, N., Müller, D., 2021. Coupled evolution of plate tectonics and basal mantle structure. Geochem. Geophys. Geosyst. 22(1), e2020GC009244.

Cawood, P.A., Korsch, R.J., 2008. Assembling Australia: Proterozoic building of a continent. Precambrian Res. 166(1-4), 1-35.

Cawood, P.A., Pisarevsky, S.A., 2017. Laurentia-Baltica-Amazonia relations during Rodinia assembly. Precambrian Res. 292, 386-397.

Cawood, P.A., Strachan, R., Cutts, K., Kinny, P.D., Hand, M., Pisarevsky, S., 2010. Neoproterozoic orogeny along the margin of Rodinia: Valhalla orogen, North Atlantic. Geology 38(2), 99-102.

Cawood, P.A., Wang, W., Zhao, T., Xu, Y., Mulder, J.A., Pisarevsky, S.A., Zhang, L., Gan, C., He, H., Liu, H., Qi, L., Wang, Y., Yao, J., Zhao, G., Zhou, M.-F., Zi, J.-W., 2020. Deconstructing South China and consequences for reconstructing Nuna and Rodinia. Earth-Sci. Rev. 204, 103169.

Chappell, B.W., White, A.J.R., 1974. Two contrasting granite types. Pacif. Geol. 8, 173-174.

Chattopadhyay, A., Bhowmik, S.K., Roy, A., 2020. Tectonothermal evolution of the Central Indian Tectonic Zone and its implications for Proterozoic supercontinent assembly: the current status. Episodes 43(1), 132-144.

Collins, A.S., Blades, M.L., Merdith, A.S., Foden, J.D., 2021. Closure of the Proterozoic Mozambique Ocean was instigated by a late Tonian plate reorganization event. Communications Earth & Environment 2(1), 75.

Collins, A.S., Pisarevsky, S.A., 2005. Amalgamating eastern Gondwana: The evolution of the Circum-Indian Orogens. Earth-Sci. Rev. 71(3-4), 229-270.

Condie, K., 2013. Preservation and recycling of crust during accretionary and collisional phases of Proterozoic Orogens: A bumpy road from Nuna to Rodinia. Geosciences 3(2), 240-261.

Condie, K.C., Pisarevsky, S.A., Puetz, S.J., 2021. LIPs, orogens and supercontinents: The ongoing saga. Gondwana Res. 96, 105-121.

Conrad, C.P., Behn, M.D., 2010. Constraints on lithosphere net rotation and asthenospheric viscosity from global mantle flow models and seismic anisotropy. Geochem. Geophys. Geosyst. 11(5), Q05W05.

Cook, F.A., Clowes, R.M., Snyder, D.B., van der Velden, A.J., Hall, K.W., Erdmer, P., Evenchick, C.A., 2004. Precambrian crust beneath the Mesozoic northern Canadian Cordillera discovered by Lithoprobe seismic reflection profiling. Tectonics 23(2), TC2010. doi:10.1029/2002TC001412

Cordani, U.G., Teixeira, W., D'Agrella-Filho, M.S., Trindade, R.I., 2009. The position of the Amazonian Craton in supercontinents. Gondwana Res. 15(3-4), 396-407.

Cox, A., Hart, R.B., 1991. Plate Tectonics: How it Works. John Wiley & Sons.

Cox, G.M., Collins, A.S., Jarrett, A.J., Blades, M.L., Shannon, A.V., Yang, B., Farkas, J., Hall, P.A., O'Hara, B., Close, D., 2022. A very unconventional hydrocarbon play: The Mesoproterozoic Velkerri Formation of northern Australia. AAPG Bulletin 106(6), 1213-1237.

Dasgupta, S., Bose, S., Das, K., 2013. Tectonic evolution of the Eastern Ghats Belt, India. Precambrian Res. 227, 247-258.

Davies, D.R., Goes, S., Sambridge, M., 2015. On the relationship between volcanic hotspot locations, the reconstructed eruption sites of large igneous provinces and deep mantle seismic structure. Earth Planet. Sci. Lett. 411, 121-130.

de Kock, M.O., Ernst, R., Söderlund, U., Jourdan, F., Hofmann, A., Le Gall, B., Bertrand, H., Chisonga, B.C., Beukes, N., Rajesh, H.M., Moseki, L.M., Fuchs, R., 2014. Dykes of the 1.11Ga Umkondo LIP, Southern Africa: Clues to a complex plumbing system. Precambrian Res. 249, 129-143.

de Kock, M.O., Evans, D.A.D., Beukes, N.J., 2009. Validating the existence of Vaalbara in the Neoarchean. Precambrian Res. 174(1-2), 145-154.

Ding, J., Zhang, S., Evans, D.A.D., Yang, T., Li, H., Wu, H., Chen, J., 2021. North China craton: The conjugate margin for northwestern Laurentia in Rodinia. Geology 49(7), 773-778.

Dobmeier, C.J., Raith, M.M., 2003. Crustal architecture and evolution of the Eastern Ghats Belt and adjacent regions of India. Geol. Soc. London Spec. Pub. 206(1), 145-168.

Domeier, M., Torsvik, T.H., 2017. Full-plate modelling in pre-Jurassic time. Geol. Mag. 156(2), 261-280.

Doughty, P.T., Chamberlain, K.R., 1996. Salmon River Arch revisited: new evidence for 1370 Ma rifting near the end of deposition in the Middle Proterozoic Belt basin. Can. J. Earth Sci. 33(7), 1037-1052.

Eglington, B.M., Pehrsson, S.J., Ansdell, K.M., Lescuyer, J.L., Quirt, D., Milesi, J.P., Brown, P., 2013. A domain-based digital summary of the evolution of the Palaeoproterozoic of North America and Greenland and associated unconformity-related uranium mineralization. Precambrian Res. 232, 4-26.

Elming, S.-Å., Mattsson, H., 2001. Post Jotnian basic intrusions in the Fennoscandian Shield, and the break up of Baltica from Laurentia: a palaeomagnetic and AMS study. Precambrian Res. 108(3-4), 215-236.

Elming, S.-Å., Salminen, J., Pesonen, L.J., 2021. Paleo-Mesoproterozoic Nuna supercycle. In: Pesonen, L.J., Salminen, J., Elming, S-A., Evans, D.A.D., Veikkolainen, T. (Eds.), Ancient Supercontinents and the Paleogeography of Earth. Elsevier, pp. 499-548.

Ernst, R.E., Hamilton, M.A., Söderlund, U., Hanes, J.A., Gladkochub, D.P., Okrugin, A.V., Kolotilina, T., Mekhonoshin, A.S., Bleeker, W., LeCheminant, A.N., Buchan, K.L., Chamberlain, K.R., Didenko, A.N., 2016. Long-lived connection between southern Siberia and northern Laurentia in the Proterozoic. Nat. Geosci. 9(6), 464-469.

Ernst, R.E., Pereira, E., Hamilton, M.A., Pisarevsky, S.A., Rodriques, J., Tassinari, C.C.G., Teixeira, W. and Van-Dunem, V., 2013. Mesoproterozoic intraplate magmatic ‘barcode’ record of the Angola portion of the Congo Craton: Newly dated magmatic events at 1505 and 1110Ma and implications for Nuna (Columbia) supercontinent reconstructions. Precambrian Res. 230, 103-118.

Evans, D., 2003. True polar wander and supercontinents. Tectonophysics: 303-320.

Evans, D.A., 2009. The palaeomagnetically viable, long-lived and all-inclusive Rodinia supercontinent reconstruction. Geol. Soc. London Spec. Pub. 327(1), 371-404.

Evans, D.A., 2013. Reconstructing pre-Pangean supercontinents. Bulletin, 125(11-12): 1735-1751.

Evans, D.A.D., 2021. Meso-Neoproterozoic Rodinia supercycle. In: Pesonen, L.J., Salminen, J., Elming, S-A., Evans, D.A.D., Veikkolainen, T. (Eds.), Ancient Supercontinents and the Paleogeography of Earth. Elsevier, pp. 549-576.

Evans, D.A.D. and Mitchell, R.N., 2011. Assembly and breakup of the core of Paleoproterozoic-Mesoproterozoic supercontinent Nuna. Geology, 39(5): 443-446.

Evans, D.A.D., Pesonen, L.J., Eglington, B.M., Elming, S.-Å., Gong, Z., Li, Z.-X., McCausland, P.J., Meert, J.G., Mertanen, S., Pisarevsky, S.A., Pivarunas, A.F., Salminen, J., Swanson-Hysell, N.L., Torsvik, T.H., Trindade, R.I.F., Veikkolainen, T., Zhang, S., 2021. An expanding list of reliable paleomagnetic poles for Precambrian tectonic reconstructions. In: Pesonen, L.J., Salminen, J., Elming, S-A., Evans, D.A.D., Veikkolainen, T. (Eds.), Ancient Supercontinents and the Paleogeography of Earth. Elsevier, pp. 605-639.

Evans, D.A.D., Veselovsky, R.V., Petrov, P.Y., Shatsillo, A.V. and Pavlov, V.E., 2016. Paleomagnetism of Mesoproterozoic margins of the Anabar Shield: A hypothesized billion-year partnership of Siberia and northern Laurentia. Precambrian Res. 281, 639-655.

Flament, N., Bodur, O.F., Williams, S.E. and Merdith, A.S., 2022. Assembly of the basal mantle structure beneath Africa. Nature, 603(7903): 846-851.

Frost, B.R., Barnes, C.G., Collins, W.J., Arculus, R.J., Ellis, D.J. and Frost, C.D., 2001. A geochemical classification for granitic rocks. Journal of petrology, 42(11): 2033-2048.

Frost, D.A. and Rost, S., 2014. The P-wave boundary of the Large-Low Shear Velocity Province beneath the Pacific. Earth Planet. Sci. Lett. 403, 380-392.

Fuck, R.A., Brito Neves, B.B. and Schobbenhaus, C., 2008. Rodinia descendants in South America. Precambrian Res. 160(1-2), 108-126.

Furlanetto, F., Thorkelson, D., Rainbird, R., Davis, W., Gibson, H. and Marshall, D., 2016. The Paleoproterozoic Wernecke Supergroup of Yukon, Canada: Relationships to orogeny in northwestern Laurentia and basins in North America, East Australia, and China. Gondwana Res. 39, 14-40.

Furlanetto, F., Thorkelson, D.J., Gibson, H.D., Marshall, D.D., Rainbird, R.H., Davis, W.J., Crowley, J.L. and Vervoort, J.D., 2013. Late Paleoproterozoic terrane accretion in northwestern Canada and the case for circum-Columbian orogenesis. Precambrian Res. 224, 512-528.

Gardiner, N.J., Maidment, D.W., Kirkland, C.L., Bodorkos, S., Smithies, R.H. and Jeon, H., 2018. Isotopic insight into the Proterozoic crustal evolution of the Rudall Province, Western Australia. Precambrian Res. 313, 31-50.

Garnero, E.J. and McNamara, A.K., 2008. Structure and dynamics of Earth's lower mantle. science, 320(5876): 626-628.

Ge, R., Zhu, W., Wilde, S.A., He, J. and Cui, X., 2015. Synchronous crustal growth and reworking recorded in late Paleoproterozoic granitoids in the northern Tarim craton: In situ zircon U-Pb-Hf-O isotopic and geochemical constraints and tectonic implications. Geological Society of America Bulletin, 127(5-6): 781-803.

Gernon, T.M., Hincks, T.K., Merdith, A.S., Rohling, E.J., Palmer, M.R., Foster, G.L., Bataille, C.P. and Müller, R.D., 2021. Global chemical weathering dominated by continental arcs since the mid-Palaeozoic. Nat. Geosci. 14(9), 690-696.

Goddéris, Y., Donnadieu, Y., Carretier, S., Aretz, M., Dera, G., Macouin, M. and Regard, V., 2017. Onset and ending of the late Palaeozoic ice age triggered by tectonically paced rock weathering. Nat. Geosci. 10(5), 382-386.

Goddéris, Y., Donnadieu, Y., Mills, B.J.W., 2023. What models tell us about the evolution of carbon sources and sinks over the Phanerozoic. Annu. Rev. Earth Planet. Sci. 51(1), 471-492.

Goodge, J.W., Fanning, C.M., Fisher, C.M., Vervoort, J.D., 2017. Proterozoic crustal evolution of central East Antarctica: Age and isotopic evidence from glacial igneous clasts, and links with Australia and Laurentia. Precambrian Res. 299, 151-176.

Gurnis, M., 1988. Large-scale mantle convection and the aggregation and dispersal of supercontinents. Nature 332(6166), 695-699.

Haines, P.W., Kirkland, C.L., Wingate, M.T.D., Allen, H., Belousova, E.A., Gréau, Y., 2016. Tracking sediment dispersal during orogenesis: A zircon age and Hf isotope study from the western Amadeus Basin, Australia. Gondwana Res. 37, 324-347.

Harley, S., 2003. Archaean-Cambrian crustal development of East Antarctica: metamorphic characteristics and tectonic implications. Geol. Soc. London Spec. Pub. 206(1), 203-230.

Harms, T.A., Brady, J.B., Burger, H.R., Cheney, J.T., 2004. Advances in the geology of the Tobacco Root Mountains, Montana, and their implications for the history of the northern Wyoming province. In: Brady, J.B., Burger, H.R., Cheney, J.T., Harms, T.A. (Eds.), Precambrian Geology of the Tobacco Root Mountains,

Montana. Boulder, Colorado, Geological Society of America Special Paper 377, p. 227–243.

Hasterok, D., Halpin, J.A., Collins, A.S., Hand, M., Kreemer, C., Gard, M.G., Glorie, S., 2022. New Maps of Global Geological Provinces and Tectonic Plates. Earth-Sci. Rev. 231, 104069.

He, Y., Zhao, G., Sun, M., Xia, X., 2009. SHRIMP and LA-ICP-MS zircon geochronology of the Xiong'er volcanic rocks: Implications for the Paleo-Mesoproterozoic evolution of the southern margin of the North China Craton. Precambrian Res. 168(3-4), 213-222.

Henderson, B., Collins, A.S., Payne, J., Forbes, C., Saha, D., 2014. Geologically constraining India in Columbia: The age, isotopic provenance and geochemistry of the protoliths of the Ongole Domain, Southern Eastern Ghats, India. Gondwana Res. 26(3-4), 888-906.

Hoffman, P.F., 1991. Did the breakout of Laurentia turn Gondwanaland inside-out? Science 252(5011), 1409-1412.

Hoffman, P.F., 1997. Tectonic genealogy of North America. In: Van der Pluijm, B.A., Marshak, S. (Eds.), Earth Structure: An Introduction to Structural Geology and Tectonics. McGraw-Hill, New York, pp. 459-464.

Hoffman, P.F., 2014. The Origin of Laurentia: Rae Craton as the Backstop for Proto-Laurentian Amalgamation by Slab Suction. Geosci. Can. 41(3), 313-320.

Holland, H.D., 2006. The oxygenation of the atmosphere and oceans. Philosophical Transactions of the Royal Society B: Biological Sciences 361(1470), 903-915.

Howard, H.M., Smithies, R.H., Kirkland, C.L., Kelsey, D.E., Aitken, A., Wingate, M.T.D., Quentin de Gromard, R., Spaggiari, C.V., Maier, W.D., 2015. The burning heart — The Proterozoic geology and geological evolution of the west Musgrave Region, central Australia. Gondwana Res. 27(1), 64-94.

Ibañez–Mejia, M., 2020. The Putumayo orogen of Amazonia: a synthesis. In: Gómez, J., Mateus–Zabala, D. (Eds.), The Geology of Colombia, Volume 1 Proterozoic – Paleozoic. Serv. Geol. Colombiano, Publicaciones Geológicas Especiales, Bogotá, 35, 101–131. https://doi.org/10.32685/pub.esp.35.2019.06.

Jacobs, J., Pisarevsky, S., Thomas, R.J., Becker, T., 2008. The Kalahari Craton during the assembly and dispersal of Rodinia. Precambrian Res. 160(1-2), 142-158.

Johansson, Å., 2009. Baltica, Amazonia and the SAMBA connection—1000 million years of neighbourhood during the Proterozoic? Precambrian Res. 175(1-4), 221-234.

Johansson, Å., Bingen, B., Huhma, H., Waight, T., Vestergaard, R., Soesoo, A., Skridlaite, G., Krzeminska, E., Shumlyanskyy, L., Holland, M.E., Holm-Denoma, C., Teixeira, W., Faleiros, F.M., Ribeiro, B.V., Jacobs, J., Wang, C., Thomas, R.J., Macey, P.H., Kirkland, C.L., Hartnady, M.I.H., Eglington, B.M., Puetz, S.J., Condie, K.C., 2022. A geochronological review of magmatism along the external margin of Columbia and in the Grenville-age orogens forming the core of Rodinia. Precambrian Res. 371, 106463.

Johnson, S.P., Sheppard, S., Rasmussen, B., Wingate, M.T.D., Kirkland, C.L., Muhling, J.R., Fletcher, I.R., Belousova, E.A., 2011. Two collisions, two sutures: Punctuated pre-1950Ma assembly of the West Australian Craton during the Ophthalmian and Glenburgh Orogenies. Precambrian Res. 189(3-4), 239-262.

Karlsen, K.S., Conrad, C.P., Magni, V., 2019. Deep water cycling and sea level change since the breakup of Pangea. Geochem. Geophys. Geosyst. 20(6), 2919-2935.

Karlstrom, K.E., Åhäll, K.-I., Harlan, S.S., Williams, M.L., McLelland, J., Geissman, J.W., 2001. Long-lived (1.8–1.0 Ga) convergent orogen in southern Laurentia, its extensions to Australia and Baltica, and implications for refining Rodinia. Precambrian Res. 111(1-4), 5-30.

Kirscher, U., Liu, Y., Li, Z.X., Mitchell, R.N., Pisarevsky, S.A., Denyszyn, S.W., Nordsvan, A., 2019. Paleomagnetism of the Hart Dolerite (Kimberley, Western Australia) – A two-stage assembly of the supercontinent Nuna? Precambrian Res. 329, 170-181.

Kirscher, U., Mitchell, R.N., Liu, Y., Nordsvan, A.R., Cox, G.M., Pisarevsky, S.A., Wang, C., Wu, L., Murphy, J.B., Li, Z.-X., 2020. Paleomagnetic constraints on the duration of the Australia-Laurentia connection in the core of the Nuna supercontinent. Geology 49(2), 174-179.

Kirscher, U., Mitchell, R.N., Liu, Y., Nordsvan, A.R., Cox, G.M., Pisarevsky, S.A., Wang, C., Wu, L., Murphy, J.B., Li, Z.-X., 2021. Paleomagnetic constraints on the duration of the Australia-Laurentia connection in the core of the Nuna supercontinent. Geology 49(2), 174-179.

Kirscher, U., Mitchell, R.N., Liu, Y., Pisarevsky, S.A., Giddings, J., Li, Z.X., 2022. Paleomagnetic evidence for a Paleoproterozoic rotational assembly of the North Australian Craton in the leadup to supercontinent formation. Geophys. Res. Lett. 49(22), e2022GL099842. https://doi.org/10.1029/2022GL099842.

Korsch, R.J., Huston, D.L., Henderson, R.A., Blewett, R.S., Withnall, I.W., Fergusson, C.L., Collins, W.J., Saygin, E., Kositcin, N., Meixner, A.J., Chopping, R., Henson, P.A., Champion, D.C., Hutton, L.J., Wormald, R., Holzschuh, J., Costelloe, R.D., 2012. Crustal architecture and geodynamics of North Queensland, Australia: Insights from deep seismic reflection profiling. Tectonophysics 572-573, 76-99.

Kulakov, E.V., Slagstad, T., Ganerød, M., Torsvik, T.H., 2022. Paleomagnetism and $^{40}Ar/^{39}Ar$ geochronology of Meso-Neoproterozoic rocks from southwest Norway. Implications for magnetic remanence ages and the paleogeography of Baltica in a Rodinia supercontinent context. Precambrian Res. 379, 106786.

Li, S., Li, X., Wang, G., Liu, Y., Wang, Z., Wang, T., Cao, X., Guo, X., Somerville, I., Li, Y., Zhou, J., Dai, L., Jiang, S., Zhao, H., Wang, Y., Wang, G., Yu, S., 2019a. Global Meso-Neoproterozoic plate reconstruction and formation mechanism for Precambrian basins: Constraints from three cratons in China. Earth-Sci. Rev. 198, 102946.

Li, S., Suo, Y., Li, X., Liu, B., Dai, L., Wang, G., Zhou, J., Li, Y., Liu, Y., Cao, X., Somerville, I., Mu, D., Zhao, S., Liu, J., Meng, F., Zhen, L., Zhao, L., Zhu, J., Yu, S., Liu, Y., Zhang, G., 2018. Microplate tectonics: new insights from micro-blocks in the global oceans, continental margins and deep mantle. Earth-Sci. Rev. 185, 1029-1064.

Li, Z.-X., Liu, Y., Ernst, R., 2023. A dynamic 2000—540 Ma Earth history: From cratonic amalgamation to the age of supercontinent cycle. Earth-Sci. Rev. 238, 104336.

Li, Z.X., Bogdanova, S.V., Collins, A.S., Davidson, A., De Waele, B., Ernst, R.E., Fitzsimons, I.C.W., Fuck, R.A., Gladkochub, D.P., Jacobs, J., Karlstrom, K.E., Lu, S., Natapov, L.M., Pease, V., Pisarevsky, S.A., Thrane, K., Vernikovsky, V., 2008. Assembly, configuration, and break-up history of Rodinia: A synthesis. Precambrian Res. 160(1-2), 179-210.

Li, Z.X., Mitchell, R.N., Spencer, C.J., Ernst, R., Pisarevsky, S., Kirscher, U., Murphy, J.B., 2019b. Decoding Earth's rhythms: Modulation of supercontinent cycles by longer superocean episodes. Precambrian Res. 323, 1-5.

Litherland, M., Power, G., 1989. The geologic and geomorphologic evolution of Serrania Huanchaca, eastern Bolivia: The legendary "Lost World". J. S. Am. Earth. Sci. 2(1), 1-17.

Liu, Q., Yu, J.-H., O'Reilly, S., Zhou, M.-F., Griffin, W., Wang, L., Cui, X., 2014. Origin and geological significance of Paleoproterozoic granites in the northeastern Cathaysia Block, South China. Precambrian Res. 248, 72-95.

Long, S., McQuarrie, N., Tobgay, T., Rose, C., Gehrels, G., Grujic, D., 2011. Tectonostratigraphy of the Lesser Himalaya of Bhutan: Implications for the along-strike stratigraphic continuity of the northern Indian margin. GSA Bulletin 123(7-8), 1406-1426.

Lubnina, N.V., Pisarevsky, S.A., Stepanova, A.V., Bogdanova, S.V., Sokolov, S.J., 2017. Fennoscandia before Nuna/Columbia: Paleomagnetism of 1.98–1.96 Ga mafic rocks of the Karelian craton and paleogeographic implications. Precambrian Res. 292, 1-12.

Macdonald, F.A., Yonkee, W.A., Flowers, R.M., Swanson-Hysell, N.L., 2023. Neoproterozoic of Laurentia. In: Whitmeyer, S.J., Williams, M.L., Kellett, D.A. and Tikoff, B. (Eds.), Laurentia: Turning Points in the Evolution of a Continent. Geological Society of America, pp. 331-380.

McQuarrie, N., Robinson, D., Long, S., Tobgay, T., Grujic, D., Gehrels, G., Ducea, M., 2008. Preliminary stratigraphic and structural architecture of Bhutan: Implications for the along strike architecture of the Himalayan system. Earth Planet. Sci. Lett. 272(1-2), 105-117.

Medig, K., Thorkelson, D., Dunlop, R., 2009. The Proterozoic Pinguicula Group: stratigraphy, contact relationships and possible correlations. Yukon Exploration and Geology, pp. 265-278.

Meert, J.G., Hargraves, R.B., Van der Voo, R., Hall, C.M., Halliday, A.N., 1994. Paleomagnetic and $^{40}Ar/^{39}Ar$ studies of late Kibaran intrusives in Burundi, East Africa: implications for late Proterozoic supercontinents. J. Geol. 102(6), 621-637.

Meert, J.G., Santosh, M., 2022. The Columbia supercontinent: Retrospective, status, and a statistical assessment of paleomagnetic poles used in reconstructions. Gondwana Res. 110, 143-164.

Merdith, A.S., Collins, A.S., Williams, S.E., Pisarevsky, S., Foden, J.D., Archibald, D.B., Blades, M.L., Alessio, B.L., Armistead, S., Plavsa, D., Clark, C., Müller, R.D., 2017a. A full-plate global reconstruction of the Neoproterozoic. Gondwana Res. 50, 84-134.

Merdith, A.S., Williams, S.E., Collins, A.S., Tetley, M.G., Mulder, J.A., Blades, M.L., Young, A., Armistead, S.E., Cannon, J., Zahirovic, S., Müller, R.D., 2021. Extending full-plate tectonic models into deep time: Linking the Neoproterozoic and the Phanerozoic. Earth-Sci. Rev. 214, 103477.

Merdith, A.S., Williams, S.E., Müller, R.D., Collins, A.S., 2017b. Kinematic constraints on the Rodinia to Gondwana transition. Precambrian Res. 299, 132-150.

Miller, C., Klötzli, U., Frank, W., Thöni, M., Grasemann, B., 2000. Proterozoic crustal evolution in the NW Himalaya (India) as recorded by circa 1.80 Ga mafic and 1.84 Ga granitic magmatism. Precambrian Res. 103(3-4), 191-206.

Mills, B.J.W., Krause, A.J., Jarvis, I., Cramer, B.D., 2023. Evolution of Atmospheric O_2 through the Phanerozoic, Revisited. Annu. Rev. Earth Planet. Sci. 51(1), 253-276.

Mitchell, R.N., Kilian, T.M., Evans, D.A., 2012. Supercontinent cycles and the calculation of absolute palaeolongitude in deep time. Nature 482(7384), 208-211.

Mitchelmore, M.D., Cook, F.A., 1994. Inversion of the Proterozoic Wernecke basin during tectonic development of the Racklan Orogen, northwest Canada. Can. J. Earth Sci. 31(3), 447-457.

Möller, C., Bingen, B., Andersson, J., Stephens, M.B., Viola, G., Scherstén, A., 2013. A non-collisional, accretionary Sveconorwegian orogen – Comment. Terra Nova 25(2), 165-168.

Morrissey, L.J., Barovich, K.M., Hand, M., Howard, K.E., Payne, J.L., 2019. Magmatism and metamorphism at ca. 1.45 Ga in the northern Gawler Craton: The Australian record of rifting within Nuna (Columbia). Geosci. Front. 10(1), 175-194.

Morrissey, L.J., Payne, J.L., Hand, M., Clark, C., Janicki, M., 2023. One billion years of tectonism at the Paleoproterozoic interface of North and South Australia. Precambrian Res. 393, 107077.

Morrissey, L.J., Payne, J.L., Hand, M., Clark, C., Taylor, R., Kirkland, C.L., Kylander-Clark, A., 2017. Linking the Windmill Islands, east Antarctica and the Albany–Fraser Orogen: Insights from U–Pb zircon geochronology and Hf isotopes. Precambrian Res. 293, 131-149.

Mukherjee, I., Large, R.R., 2020. Co-evolution of trace elements and life in Precambrian oceans: The pyrite edition. Geology 48(10), 1018-1022.

Mulder, J.A., Karlstrom, K.E., Halpin, J.A., Merdith, A.S., Spencer, C.J., Berry, R.F., McDonald, B., 2018. Rodinian devil in disguise: Correlation of 1.25–1.10 Ga strata between Tasmania and Grand Canyon. Geology 46(11), 991-994.

Müller, R.D., Cannon, J., Qin, X., Watson, R.J., Gurnis, M., Williams, S., Pfaffelmoser, T., Seton, M., Russell, S.H.J., Zahirovic, S., 2018. GPlates: Building a virtual Earth through deep time. Geochem. Geophys. Geosyst. 19(7), 2243-2261.

Müller, R.D., Flament, N., Cannon, J., Tetley, M.G., Williams, S.E., Cao, X., Bodur, Ö.F., Zahirovic, S., Merdith, A., 2022a. A tectonic-rules-based mantle reference frame since 1 billion years ago – implications for supercontinent cycles and plate–mantle system evolution. Solid Earth 13(7), 1127-1159.

Müller, R.D., Mather, B., Dutkiewicz, A., Keller, T., Merdith, A., Gonzalez, C.M., Gorczyk, W., Zahirovic, S., 2022b. Evolution of Earth's tectonic carbon conveyor belt. Nature 605(7911), 629-639.

Müller, R.D., Seton, M., Zahirovic, S., Williams, S.E., Matthews, K.J., Wright, N.M., Shephard, G.E., Maloney, K.T., Barnett-Moore, N., Hosseinpour, M., Bower, D.J., Cannon, J., 2016. Ocean basin evolution and global-scale plate reorganization events since Pangea breakup. Annu. Rev. Earth Planet. Sci. 44(1), 107-138.

Murphy, J.B., Nance, R.D., 2003. Do supercontinents introvert or extrovert?: Sm-Nd isotope evidence. Geology 31(10), 873-876.

Nance, R.D., Murphy, J.B., Santosh, M., 2014. The supercontinent cycle: A retrospective essay. Gondwana Res. 25(1), 4-29.

Nixon, A.L., Glorie, S., Collins, A.S., Blades, M.L., Simpson, A., Whelan, J.A., 2022. Inter-cratonic geochronological and geochemical correlations of the Derim Derim–Galiwinku/Yanliao reconstructed Large Igneous Province across the North Australian and North China cratons. Gondwana Res. 103, 473-486.

Nordsvan, A.R., Collins, W.J., Li, Z.-X., Spencer, C.J., Pourteau, A., Withnall, I.W., Betts, P.G., Volante, S., 2018. Laurentian crust in northeast Australia: Implications for the assembly of the supercontinent Nuna. Geology 46(3), 251-254.

Occhipinti, S.A., Sheppard, S., Passchier, C., Tyler, I.M., Nelson, D.R., 2004. Palaeoproterozoic crustal accretion and collision in the southern Capricorn Orogen: the Glenburgh Orogeny. Precambrian Res. 128(3-4), 237-255.

Park, R., 1992. Plate kinematic history of Baltica during the Middle to Late Proterozoic: a model. Geology 20(8), 725-728.

Park, Y., Swanson‐Hysell, N.L., Xian, H., Zhang, S., Condon, D.J., Fu, H., Macdonald, F.A., 2021. A consistently high‐latitude South China from 820 to 780 Ma: Implications for exclusion from Rodinia and the feasibility of large‐scale true polar wander. J. Geophys. Res.: Solid Earth 126(6), e2020JB021541.

Pehrsson, S.J., Eglington, B.M., Evans, D.A.D., Huston, D., Reddy, S.M., 2016. Metallogeny and its link to orogenic style during the Nuna supercontinent cycle. Geol. Soc. London Spec. Pub. 424(1), 83-94.

Pesonen, L., Elming, S.-Å., Mertanen, S., Pisarevsky, S., D'Agrella-Filho, M., Meert, J., Schmidt, P., Abrahamsen, N., Bylund, G., 2003. Palaeomagnetic configuration of continents during the Proterozoic. Tectonophysics 375(1-4), 289-324.

Pisarevsky, S., Bylund, G., 2010. Paleomagnetism of 1780–1770 Ma mafic and composite intrusions of Småland (Sweden): implications for the Mesoproterozoic supercontinent. Am. J. Sci. 310(9), 1168-1186.

Pisarevsky, S., Natapov, L., 2003. Siberia and rodinia. Tectonophysics 375(1-4), 221-245.

Pisarevsky, S., Natapov, L., Donskaya, T., Gladkochub, D., Vernikovsky, V., 2008. Proterozoic Siberia: a promontory of Rodinia. Precambrian Res. 160(1-2), 66-76.

Pisarevsky, S.A., Biswal, T.K., Wang, X.-C., De Waele, B., Ernst, R., Söderlund, U., Tait, J.A., Ratre, K., Singh, Y.K., Cleve, M., 2013. Palaeomagnetic, geochronological and geochemical study of Mesoproterozoic Lakhna Dykes in the Bastar Craton, India: Implications for the Mesoproterozoic supercontinent. Lithos 174, 125-143.

Pisarevsky, S.A., Elming, S.-Å., Pesonen, L.J., Li, Z.-X., 2014. Mesoproterozoic paleogeography: Supercontinent and beyond. Precambrian Res. 244, 207-225.

Pisarevsky, S.A., Gladkochub, D.P., Donskaya, T.V., 2021. Chapter 8: Precambrian paleogeography of Siberia. In: Pesonen, L.J., Salminen, J., Elming, S-

A., Evans, D.A.D., Veikkolainen, T. (Eds.), Ancient Supercontinents and the Paleogeography of Earth. Elsevier, pp. 263-275.

Pisarevsky, S.A., Li, Z.X., Tetley, M.G., Liu, Y., Beardmore, J.P., 2022. An updated internet-based Global Paleomagnetic Database. Earth-Sci. Rev. 235, 104258.

Pisarevsky, S.A., Wingate, M.T., Powell, C.M., Johnson, S., Evans, D.A., 2003. Models of Rodinia assembly and fragmentation. Geol. Soc. London Spec. Pub. 206(1), 35-55.

Pourteau, A., Smit, M.A., Li, Z., Collins, W.J., Nordsvan, A.R., Volante, S., Li, J., 2018. 1.6 Ga crustal thickening along the final Nuna suture. Geology 46(11), 959-962.

Rawlings, D., 1999. Stratigraphic resolution of a multiphase intracratonic basin system: the McArthur Basin, northern Australia. Aust. J. Earth Sci. 46(5), 703-723.

Richards, A., Argles, T., Harris, N., Parrish, R., Ahmad, T., Darbyshire, F., Draganits, E., 2005. Himalayan architecture constrained by isotopic tracers from clastic sediments. Earth Planet. Sci. Lett. 236(3-4), 773-796.

Rickers, K., Mezger, K., Raith, M.M., 2001. Evolution of the continental crust in the Proterozoic Eastern Ghats Belt, India and new constraints for Rodinia reconstruction: implications from Sm–Nd, Rb–Sr and Pb–Pb isotopes. Precambrian Res. 112(3-4), 183-210.

Rivers, T., 2008. Assembly and preservation of lower, mid, and upper orogenic crust in the Grenville Province—Implications for the evolution of large hot long-duration orogens. Precambrian Res. 167(3-4), 237-259.

Rivers, T., 2015. Tectonic setting and evolution of the Grenville Orogen: An assessment of progress over the last 40 years. Geosci. Can. 42(1), 77-124.

Roberts, N., Condie, K., Palin, R., Spencer, C., 2023. Hot, wide, continental back-arcs explain Earth's enigmatic mid-Proterozoic magmatic and metamorphic record. Tektonika 1(1), 67-75.

Roberts, N.M., Salminen, J., Johansson, Å., Mitchell, R.N., Palin, R.M., Condie, K.C., Spencer, C.J., 2022. On the enigmatic mid-Proterozoic: Single-lid versus plate tectonics. Earth Planet. Sci. Lett. 594, 117749.

Roberts, N.M.W., 2013. The boring billion? – Lid tectonics, continental growth and environmental change associated with the Columbia supercontinent. Geosci. Front. 4(6), 681-691.

Rogers, J.J.W., Santosh, M., 2002. Configuration of Columbia, a Mesoproterozoic supercontinent. Gondwana Res. 5(1), 5-22.

Ross, G., Villeneuve, M., Theriault, R., 2001. Isotopic provenance of the lower Muskwa assemblage (Mesoproterozoic, Rocky Mountains, British Columbia): New clues to correlation and source areas. Precambrian Res. 111(1-4), 57-77.

Ross, G.M., Parrish, R.R., Winston, D., 1992. Provenance and U-Pb geochronology of the Mesoproterozoic Belt Supergroup (northwestern United States): Implications for age of deposition and pre-Panthalassa plate reconstructions. Earth Planet. Sci. Lett. 113(1-2), 57-76.

Salminen, J., Hanson, R., Evans, D.A.D., Gong, Z., Larson, T., Walker, O., Gumsley, A., Söderlund, U., Ernst, R., 2018. Direct Mesoproterozoic connection of the Congo and Kalahari cratons in proto-Africa: Strange attractors across supercontinental cycles. Geology 46(11), 1011-1014.

Salminen, J., Pesonen, L.J., 2007. Paleomagnetic and rock magnetic study of the Mesoproterozoic sill, Valaam island, Russian Karelia. Precambrian Res. 159(3-4), 212-230.

Salminen, J., Pesonen, L.J., Mertanen, S., Vuollo, J., Airo, M.-L., 2009. Palaeomagnetism of the Salla Diabase Dyke, northeastern Finland, and its implication for the Baltica-Laurentia entity during the Mesoproterozoic. Geol. Soc. London Spec. Pub. 323(1), 199-217.

Santos, J.O.S., Hartmann, L.A., Gaudette, H.E., Groves, D.I., Mcnaughton, N.J., Fletcher, I.R., 2000. A new understanding of the provinces of the Amazon Craton based on integration of field mapping and U-Pb and Sm-Nd geochronology. Gondwana Res. 3(4), 453-488.

Seton, M., Müller, R.D., Zahirovic, S., Gaina, C., Torsvik, T., Shephard, G., Talsma, A., Gurnis, M., Turner, M., Maus, S., Chandler, M., 2012. Global continental and ocean basin reconstructions since 200 Ma. Earth-Sci. Rev. 113(3-4), 212-270.

Seton, M., Williams, S.E., Domeier, M., Collins, A.S., Sigloch, K., 2023. Deconstructing plate tectonic reconstructions. Nature Reviews Earth & Environment 4(3), 185-204.

Slagstad, T., Kulakov, E., Kirkland, C.L., Roberts, N.M.W., Ganerød, M., 2019. Breaking the Grenville–Sveconorwegian link in Rodinia reconstructions. Terra Nova 31(5), 430-437.

Slagstad, T., Kulakov, E.V., Anderson, M.W., Saalmann, K., Kirkland, C.L., Henderson, I.H.C., Ganerød, M., 2023. Was Baltica part of Rodinia? Terra Nova 35(3), 167-173.

Slagstad, T., Roberts, N.M.W., Marker, M., Røhr, T.S., Schiellerup, H., 2012. A non-collisional, accretionary Sveconorwegian orogen. Terra Nova 25(1), 30-37.

Spaggiari, C.V., Smithies, R.H., Kirkland, C.L., Wingate, M.T.D., England, R.N., Lu, Y.-J., 2018. Buried but preserved: The Proterozoic Arubiddy Ophiolite, Madura Province, Western Australia. Precambrian Res. 317, 137-158.

Spencer, C.J., 2022. Biogeodynamics: Coupled evolution of the biosphere, atmosphere, and lithosphere. Geology 50(8), 867-868.

Starmer, I.C., 1996. Accretion, rifting, rotation and collision in the North Atlantic supercontinent, 1700-950 Ma. Geol. Soc. London Spec. Pub. 112(1), 219-248.

Stern, R., 2020. The Mesoproterozoic single-lid tectonic episode: Prelude to modern plate tectonics. GSA Today 30(12):, 4-10.

Swanson-Hysell, N.L., 2021. The Precambrian paleogeography of Laurentia. In: Pesonen, L.J., Salminen, J., Elming, S-A., Evans, D.A.D., Veikkolainen, T. (Eds.), Ancient Supercontinents and the Paleogeography of Earth. Elsevier, pp. 109-153.

Swanson-Hysell, N.L., Kilian, T.M., Hanson, R.E., 2015. A new grand mean palaeomagnetic pole for the 1.11 Ga Umkondo large igneous province with implications for palaeogeography and the geomagnetic field. Geophys. J. Int. 203(3), 2237-2247.

Swanson-Hysell, N.L., Ramezani, J., Fairchild, L.M., Rose, I.R., 2019. Failed rifting and fast drifting: Midcontinent Rift development, Laurentia's rapid motion and the driver of Grenvillian orogenesis. GSA Bulletin 131(5-6), 913-940.

Tamblyn, R., Hasterok, D., Hand, M., Gard, M., 2021. Mantle heating at ca. 2 Ga by continental insulation: Evidence from granites and eclogites. Geology 50(1), 91-95.

Thorkelson, D.J., Abbott, J.G., Mortensen, J.K., Creaser, R.A., Villeneuve, M.E., McNicoll, V.J., Layer, P.W., 2005. Early and middle Proterozoic evolution of Yukon, Canada. Can. J. Earth Sci. 42(6), 1045-1071.

Thorkelson, D.J., Mortensen, J.K., Creaser, R.A., Davidson, G.J., Abbott, J.G., 2001. Early Proterozoic magmatism in Yukon, Canada: constraints on the evolution of northwestern Laurentia. Can. J. Earth Sci. 38(10), 1479-1494.

Tohver, E., Pluijm, B.A.v.d., Mezger, K., Scandolara, J.E., Essene, E.J., 2005a. Two stage tectonic history of the SW Amazon craton in the late Mesoproterozoic: identifying a cryptic suture zone. Precambrian Res. 137(1-2), 35-59.

Tohver, E., Van Der Pluijm, B., Scandolara, J., Essene, E., 2005b. Late Mesoproterozoic deformation of SW Amazonia (Rondônia, Brazil): geochronological and structural evidence for collision with southern Laurentia. J. Geol. 113(3), 309-323.

Tohver, E., Van der Pluijm, B., Van der Voo, R., Rizzotto, G., Scandolara, J., 2002. Paleogeography of the Amazon craton at 1.2 Ga: early Grenvillian collision with the Llano segment of Laurentia. Earth Planet. Sci. Lett. 199(1-2), 185-200.

Torsvik, T.H., Burke, K., Steinberger, B., Webb, S.J., Ashwal, L.D., 2010. Diamonds sampled by plumes from the core-mantle boundary. Nature 466(7304), 352-355.

Torsvik, T.H., Cocks, L.R.M., 2017. The integration of palaeomagnetism, the geological record and mantle tomography in the location of ancient continents. Geol. Mag. 156(2), 242-260.

Upton, B., Rämö, O.T., Heaman, L., Blichert-Toft, J., Kalsbeek, F., Barry, T., Jepsen, H., 2005. The Mesoproterozoic Zig-Zag Dal basalts and associated intrusions of eastern North Greenland: mantle plume–lithosphere interaction. Contrib. Mineral. Petrol. 149, 40-56.

Van der Voo, R., 1990. The reliability of paleomagnetic data. Tectonophysics 184(1), 1-9.

Volante, S., Pourteau, A., Collins, W.J., Blereau, E., Li, Z.X., Smit, M., Evans, N.J., Nordsvan, A.R., Spencer, C.J., McDonald, B.J., Li, J., Günter, C., 2020. Multiple P–T–d–t paths reveal the evolution of the final Nuna assembly in northeast Australia. J. Metamorph. Geol. 38(6), 593-627.

Wang, C., Li, Z.X., Peng, P., Pisarevsky, S., Liu, Y., Kirscher, U., Nordsvan, A., 2019. Long-lived connection between the North China and North Australian cratons in supercontinent Nuna: paleomagnetic and geological constraints. Sci. Bull. 64(13), 873-876.

Wang, C., Mitchell, R.N., Murphy, J.B., Peng, P., Spencer, C.J., 2020a. The role of megacontinents in the supercontinent cycle. Geology 49(4), 402-406.

Wang, L.-J., Yu, J.-H., Griffin, W., O'Reilly, S., 2012. Early crustal evolution in the western Yangtze Block: evidence from U–Pb and Lu–Hf isotopes on detrital zircons from sedimentary rocks. Precambrian Res. 222, 368-385.

Wang, P., Zhao, G., Liu, Q., Han, Y., Yao, J., Li, J., 2020b. Zircons from the Tarim basement provide insights into its positions in Columbia and Rodinia supercontinents. Precambrian Res. 341, 105621.

Wang, W., Cawood, P.A., Pandit, M.K., 2021. India in the Nuna to Gondwana supercontinent cycles: Clues from the north Indian and Marwar Blocks. Am. J. Sci. 321(1-2), 83-117.

Wang, W., Cawood, P.A., Zhou, M.-F., Zhao, J.-H., 2016. Paleoproterozoic magmatic and metamorphic events link Yangtze to northwest Laurentia in the Nuna supercontinent. Earth Planet. Sci. Lett. 433, 269-279.

Wang, W., Zhou, M.-F., 2014. Provenance and tectonic setting of the Paleo-to Mesoproterozoic Dongchuan Group in the southwestern Yangtze Block, South China: implication for the breakup of the supercontinent Columbia. Tectonophysics 610, 110-127.

Weller, O.M., Mottram, C.M., St-Onge, M.R., Möller, C., Strachan, R., Rivers, T., Copley, A., 2021. The metamorphic and magmatic record of collisional orogens. Nature Reviews Earth & Environment 2(11), 781-799.

Whitmeyer, S.J., Karlstrom, K.E., 2007. Tectonic model for the Proterozoic growth of North America. Geosphere 3(4), 220-259.

Williams, H., Hoffman, P.F., Lewry, J.F., Monger, J.W., Rivers, T., 1991. Anatomy of North America: thematic geologic portrayals of the continent. Tectonophysics 187(1-3), 117-134.

Wrobel-Daveau, J.-C., Nicoll, G., Tetley, M.G., Gréselle, B., Perez-Diaz, L., Davies, A., Eglington, B.M., 2022. Plate tectonic modelling and the energy transition. Earth-Sci. Rev. 234, 104227.

Xu, Y.-J., Cawood, P.A., Du, Y.-S., 2016. Intraplate orogenesis in response to Gondwana assembly: Kwangsian orogeny, South China. Am. J. Sci. 316(4), 329-362.

Yang, B., Collins, A.S., Blades, M.L., Jourdan, F., 2023. Orogens and detritus: unravelling the Mesoproterozoic tectonic geography of northern Australia through coupled detrital thermo- and geo-chronometers. Aust. J. Earth Sci. 1-19.

Yang, B., Collins, A.S., Blades, M.L., Munson, T.J., Payne, J.L., Glorie, S., Farkaš, J., 2020. Tectonic controls on sedimentary provenance and basin geography of the Mesoproterozoic Wilton package, McArthur Basin, northern Australia. Geol. Mag. 159(2), 179-198.

Yao, J., Cawood, P.A., Shu, L., Zhao, G., 2019. Jiangnan Orogen, South China: A ~970–820 Ma Rodinia margin accretionary belt. Earth-Sci. Rev. 196, 102872.

Yao, W., Li, Z.-X., Li, W.-X., Li, X.-H., 2017. Proterozoic tectonics of Hainan Island in supercontinent cycles: New insights from geochronological and isotopic results. Precambrian Res. 290, 86-100.

Young, A., Flament, N., Maloney, K., Williams, S., Matthews, K., Zahirovic, S., Müller, R.D., 2019. Global kinematics of tectonic plates and subduction zones since the late Paleozoic Era. Geosci. Front. 10(3), 989-1013.

Yu, J.-H., O'Reilly, S.Y., Zhou, M.-F., Griffin, W., Wang, L., 2012. U–Pb geochronology and Hf–Nd isotopic geochemistry of the Badu Complex, Southeastern China: implications for the Precambrian crustal evolution and paleogeography of the Cathaysia Block. Precambrian Res. 222, 424-449.

Yu, J.-H., Wang, L., O'reilly, S., Griffin, W., Zhang, M., Li, C., Shu, L., 2009. A Paleoproterozoic orogeny recorded in a long-lived cratonic remnant (Wuyishan terrane), eastern Cathaysia Block, China. Precambrian Res. 174(3-4), 347-363.

Zahirovic, S., Müller, R.D., Seton, M., Flament, N., 2015. Tectonic speed limits from plate kinematic reconstructions. Earth Planet. Sci. Lett. 418, 40-52.

Zhang, N., Zhong, S., Leng, W., Li, Z., 2010. A model for the evolution of the Earth's mantle structure since the Early Paleozoic. J. Geophys. Res. 115(B6), B06401.

Zhang, S., Li, Z.-X., Evans, D.A.D., Wu, H., Li, H., Dong, J., 2012. Pre-Rodinia supercontinent Nuna shaping up: A global synthesis with new paleomagnetic results from North China. Earth Planet. Sci. Lett. 353-354, 145-155.

Zhang, S.-H., Ernst, R.E., Yang, Z., Zhou, Z., Pei, J., Zhao, Y., 2022. Spatial distribution of 1.4-1.3 Ga LIPs and carbonatite-related REE deposits: Evidence for large-scale continental rifting in the Columbia (Nuna) supercontinent. Earth Planet. Sci. Lett. 597, 117815.

Zhang, S.-H., Zhao, Y., Li, X.-H., Ernst, R.E., Yang, Z.-Y., 2017. The 1.33–1.30 Ga Yanliao large igneous province in the North China Craton: Implications for reconstruction of the Nuna (Columbia) supercontinent, and specifically with the North Australian Craton. Earth Planet. Sci. Lett. 465, 112-125.

Zhao, G., Cawood, P.A., Wilde, S.A., Sun, M., 2002. Review of global 2.1–1.8 Ga orogens: implications for a pre-Rodinia supercontinent. Earth-Sci. Rev. 59(1-4), 125-162.

Zhao, L., Tyler, I.M., Gorczyk, W., Murdie, R.E., Gessner, K., Lu, Y., Smithies, H., Li, T., Yang, J., Zhan, A., 2022. Seismic evidence of two cryptic sutures in Northwestern Australia: Implications for the style of subduction during the Paleoproterozoic assembly of Columbia. Earth Planet. Sci. Lett. 579, 117342.

Zhao, T., Cawood, P.A., Zi, J.-W., Wang, K., Feng, Q., Tran, D.M., Trinh, H.D., Dang, C.M., Nguyen, Q.M., 2023. Positioning the Yangtze Block within Nuna: Constraints from Paleoproterozoic granitoids in North Vietnam. Precambrian Res. 391, 107059.

Zhu, Z., Campbell, I.H., Allen, C.M., Brocks, J.J., Chen, B., 2022. The temporal distribution of Earth's supermountains and their potential link to the rise of atmospheric oxygen and biological evolution. Earth Planet. Sci. Lett. 580, 117391.

Zou, Y., Mitchell, R.N., Chu, X., Brown, M., Jiang, J., Li, Q., Zhao, L., Zhai, M., 2023. Surface evolution during the mid-Proterozoic stalled by mantle warming under Columbia–Rodinia. Earth Planet. Sci. Lett. 607, 118055.

Figure captions

Fig. 1. (a) Major cratonic blocks used in the reconstructions before 1.0 Ga; (b) The three base models used in this study. The continental outlines in (a) are modified from Merdith et al. (2021). The grey lines in (b) show the timespan of each base model. Our refinements to the base models are mainly for pre-1.0 Ga times, with minor changes for the Neoproterozoic. The new model includes three supercontinents: Nuna, Rodinia and Pangea. LAU-Laurentia, AMA-Amazonia, SF-São Francisco, BAL-Baltica, RAY-Rayner Province, MAW-Mawson, SA-South Australia, NA-North Australia, WA-West Australia, YA-Yangtze, CA-Cathaysia, NC-North China, SIB-Siberia, TA-Tarim, SI-South India, NI-North India, CON-Congo, KAL-Kalahari, WAF-West Africa, SAH-Sahara Metacraton.

Fig. 2. Temporal distribution of the paleomagnetic poles used in this study. The poles are compiled from the GPMDB database (http://gpmdb.net; Pisarevsky et al., 2022). Baltica here indicates eastern Baltica (i.e. Sarmatia/Volgo-Uralia) before 1.7 Ga and the whole of Baltica (Sarmatia/Volgo-Uralia and Fennocandia) afterwards. The error bars show the age uncertainties of the poles.

Fig. 3. Point data used for identifying plate boundary type. (a) Igneous rocks of both I-type and magnesian-type (high magnesium to iron ratios) of FeO/(FeO+MgO) classification from Frost et al. (2001), (b) metamorphic gradients with age constraints, circles indicate high gradients (>775 K/Gpa), triangles indicate medium values (375-775 K/Gpa), and diamonds indicate low values (<375 K/Gpa). The continental outlines are modified from Merdith et al. (2021). See supplementary model files for details.

Fig. 4. Accretionary events along the margins of major cratonic blocks between 1.8 Ga and 1.0 Ga. The texts in brackets after cratonic block names denote along which margin (in present-day coordinates) the accretionary events occurred. The data are mainly from Condie et al. (2021) with minor changes (see Supplementary Data Table S2). The numbers above the lines denote tectonic event numbers listed in Supplementary Data Table S2. There are overlaps between different tectonic events indicating they occur in different segments of the margin, or due to age uncertainties.

Fig. 5. The configuration of supercontinent Nuna (1580 Ma) in P14 and in this study. India is separated into the North Indian and South Indian blocks; Yangtze, Cathaysia and Tarim are added to our model; The positions of Siberia, Kalahari, North China, West Australia are adjusted based on paleomagnetic and geological data. See Fig. 1 for abbreviations.

Fig. 6. Evolution of Laurentia and surrounding blocks during Nuna assembly in P14 and in this study. The plate positions are adjusted to better align with paleomagnetic data. Poles and continents with the same plate ID are shown with the same colors. See Fig. 1 for abbreviations.

Fig. 7. (a) Motion path and (b) rate of motion of Laurentia in P14 and in this study. The motion of Laurentia is smoother and slower in this study compared with P14. See Fig. 1 for abbreviations. The transparent yellow-green bar represents the period during which supercontinent Nuna existed.

Fig. 8. Evolution of East Nuna in P14 and in this study. The plate configurations are adjusted to better align with paleomagnetic and geological data. Poles and continents with the same plate ID are shown with the same colors. See Fig. 1 for abbreviations.

Fig. 9. Tectonic evolution of Amazonia-West Africa in P14 and in this study. The two blocks are inferred to be located within a large ocean basin, distal to other continents from 1.8 Ga to 1.0 Ga. Their paleolatitude is constrained by paleomagnetic data. See Fig. 1 for abbreviations.

Fig. 10. West Africa-Amazonia configuration in Merdith et al. (2021, left) and in this study (right). West Africa is rotated relative to Amazonia based on a pole (the light blue circle, pole No. 9968; Antonio et al., 2021) at 860 Ma. Poles and continents with the same plate ID are shown with the same colors. See Fig. 1 for abbreviations.

Fig. 11. Comparison of the breakup of Nuna in C21 and in this study. The breakup initiates at 1.46 Ga from the north and progresses southward in our model. The rift history of the Australian blocks is largely adopted from P14 and C21, while other blocks are significantly refined or new modelled using available data. See Fig. 1 for abbreviations.

Fig. 12. Breakup of West Africa and Amazonia in M21 (left) and in this study (right). The rift timing of West Africa from Laurentia and Amazonia is adjusted from 850 Ma in M21 to 720 Ma in our model, followed by the accretion onto the Sahara Metacraton at 600 Ma following M21. See Fig. 1 for abbreviations.

Fig. 13. Global plate reconstructions between 1800 Ma and 900 Ma. The red numbers denote tectonic event numbers shown in Fig. 4 and Supplementary Data Table S2. The model starts with a quasi-supercontinent at 1.8 Ga. The East, West, and South Nuna merged at 1.6 Ga, causing the Racklan/Isan orogeny. The breakup of Nuna primarily occurred between ca. 1.46-1.3 Ga. After the breakup of Nuna, the continental blocks came back together at 930 Ma, forming Rodinia. West Africa and Amazonia stayed in the ocean to the west of Nuna from 1800 Ma until their collision with Laurentia at 1070 Ma. See Fig. 1 for abbreviations.

Fig. 14. Fit of palaeomagnetic data to our model. The misfit is defined as the minimum great circle distance between the North Pole and the reconstructed palaeomagnetic pole within the valid time range (Merdith et al., 2021). The misfit between the paleomagnetic poles and our reconstructions are generally below 25°, with a mean of around 12°, which is similar to the misfit in M21 for the last 1 Gyr. The solid line denotes the mean misfit of all poles, and the dashed lines denote the corresponding standard deviation. The error bars denote 95% confidence limits (A95).

Fig. 15. Geometric and kinematic characteristics of our plate reconstruction. (a) Ridge and subduction zone length through time, the mid-ocean ridge length shows cyclic evolution similar to supercontinents; (b) Net lithospheric rotation and RMS speeds of all plates, they display similar trends. The transparent yellow-green bars denote the durations of the supercontinents' existence.

Supplementary Data

Supplementary Data Fig. S1. Fit of palaeomagnetic data for each continental block in P14 and in this study. The misfit is defined as the minimum great circle distance between the north pole and the reconstructed palaeomagnetic pole within the valid time range. The mean misfit for all plates was equal to 19° in P14 and is equal to 12° in our model. The smaller misfit in our model is partly attributed to the inclusion of poles published since P14 was published. The error bars denote the standard deviation of the mean values.

Supplementary Data Fig. S2. Reconstructed point data. Metamorphic gradients: magenta circles indicate high gradients (>775 K/Gpa), yellow circles indicate medium values (375-775 K/Gpa), and red circles indicate low values (<375 K/Gpa). Green triangles indicate igneous rocks of both I-type and magnesian-type (high magnesium to iron ratios) of FeO/FeO+MgO classification from Frost et al. (2001).

Supplementary Data Table S1. Selected Proterozoic paleomagnetic poles. SLAT-site latitude, SLONG-site longitude, PLAT-pole latitude, PLONG-pole longitude.

Supplementary Data Table S2. Accretionary events along the margins of major cratonic blocks

Highlights:

- We present a full-plate tectonic model for the last 1.8 Gyr.
- The model is constrained by geological and geophysical data.
- It spans three supercontinents and forms the basis for future Earth system studies.